

Vacuum type space-like string surfaces in $\text{AdS}_3 \times \text{S}^3$

Harald Dorn,^a George Jorjadze,^{a,b} Chrysostomos Kalousios,^a
Luka Megrelidze,^c Sebastian Wuttke^{a †}

^a*Institut für Physik der Humboldt-Universität zu Berlin,
Newtonstraße 15, D-12489 Berlin, Germany*

^b*Razmadze Mathematical Institute,
M. Aleksidze 1, 0193, Tbilisi, Georgia*

^c*Ilia State University,
K. Cholokashvili Ave 3/5, 0162, Tbilisi, Georgia*

Abstract

We construct and classify all space-like minimal surfaces in $\text{AdS}_3 \times \text{S}^3$ which globally admit coordinates with constant induced metric on both factors. Up to $\text{O}(2, 2) \times \text{O}(4)$ transformations all these surfaces, except one class, are parameterized by four real parameters. The classes of surfaces correspond to different regions in this parameter space and show quite different boundary behavior. Our analysis uses a direct construction of the string coordinates via a group theoretical treatment based on the map of $\text{AdS}_3 \times \text{S}^3$ to $\text{SL}(2, \mathbb{R}) \times \text{SU}(2)$. This is complemented by a cross check via standard Pohlmeyer reduction. After embedding in $\text{AdS}_5 \times \text{S}^5$ we calculate the regularized area for solutions with a boundary spanned by a four point scattering s -channel momenta configuration.

[†]{dorn,jorj,ckalousi,wuttke}@physik.hu-berlin.de

Contents

1	Introduction	1
2	Space-like strings in $\mathrm{SL}(2, \mathbb{R}) \times \mathrm{SU}(2)$	3
2.1	AdS ₃ and S ³ as group manifolds	3
2.2	String description in terms of group variables	4
2.3	Vacuum solutions in SU(2)	5
2.4	Vacuum solutions in SL(2, ℝ)	9
3	Analysis via Pohlmeyer reduction	19
3.1	Time-like AdS ₃ projection	19
3.2	Integration of the linear system	21
3.3	Light-like AdS ₃ projection	23
3.4	Relation to complex sin(h)-Gordon models	25
4	Analysis of the boundaries	26
5	Embedding in AdS₅ and a regularized area	30
6	Conclusions	33
A	Useful formulæ	34
A.1	SU(2) group	34
A.2	SL(2, ℝ) group	35
B	Left-right decomposition of $\mathfrak{so}(2, 2)$	35

1 Introduction

In a series of papers [1, 2] a remarkable correspondence between minimal surfaces in AdS₅ approaching a null polygonal boundary at conformal infinity and gluon scattering amplitudes in $\mathcal{N} = 4$ super Yang-Mills theory has been established. For generic null polygons a lot of structural insight concerning the dependence of the area on the boundary data has been achieved. However, explicit formulæ for the surfaces are available in the tetragon case only [3, 1]. The tetragon case is very special, since it turned out to be the only flat space-like minimal surface in AdS₅ [4].

The string dual to $\mathcal{N} = 4$ SYM lives in AdS₅ × S⁵. There is an extensive literature on dynamical strings, i.e. time-like surfaces, in AdS × S (see for example [5] and references

therein). For the correspondence to scattering amplitudes one is interested in space-like surfaces extended up to infinity. Therefore, a more complete treatment should include the study of minimal surfaces in this ten-dimensional spacetime with the same null polygonal boundaries for their projection on AdS_5 , but with a non-trivial extension in S^5 . We started a corresponding analysis for $\text{AdS}_3 \times S^3$ in [6]. For an example in $\text{AdS}_3 \times S^1$ see [7]. The situation now exhibits two crucial new aspects. While at first the surface in the total product space of course has to be minimal, its projections to the factors can be non-minimal. Secondly, surfaces which are space-like with respect to the induced metric of the full product space can have projections to AdS of both Euclidean and Lorentzian signature or even with a degenerate induced metric. In [6] we concentrated on the case of a space-like AdS-projection and made only some sketchy remarks on the time-like case. Allowing non-space-like AdS-projections opens a relatively broad set of possibilities. The present paper is devoted to a full constructive classification within the set of surfaces which admit coordinates where the metrics induced from the product space as well as from the individual factors are constant¹.

The by now standard procedure for generating minimal surfaces as the solution of string equations of motion is Pohlmeyer reduction [8, 4]. The reduced model inherits possible integrable structures of the original string sigma model. After solving the reduced model a first order linear problem has still to be solved to get the coordinates of the wanted surfaces. Based on the bijective maps of AdS_3 and S^3 to the group manifolds $\text{SL}(2, \mathbb{R})$ and $\text{SU}(2)$, respectively, we perform an analysis which yields the embedding coordinates directly. The analysis of AdS_3 string equations in terms of $\text{SL}(2, \mathbb{R})$ group variables is usually very helpful for the dynamics with WZ term (see [9, 10] and references therein). It appears that the vacuum configurations of $\text{AdS}_3 \times S^3$ string also have a certain factorized structure, which provides explicit integration of corresponding string equations. For completeness and a cross check we also analyze the problem in Pohlmeyer reduction.

The paper is organized as follows. In section 2 we review the map to a group manifold and then classify and construct the solutions of vacuum type corresponding to space-like surfaces in $\text{AdS}_3 \times S^3$. We show that three left and three right components of Noether currents related to the isometries of $\text{SL}(2, \mathbb{R}) \times \text{SU}(2)$ are constants both in AdS_3 and S^3 sectors. That also justifies the name vacuum type solutions. Section 3 is devoted to a parallel treatment of the problem within Pohlmeyer reduction. In addition it contains remarks on the relation of our solutions to the complex $\sin(\mathfrak{h})$ -Gordon type equations, which for the light-like AdS_3 projection degenerate to a linear equation. Then we continue in section 4 with an elaboration of the boundary behavior of our surfaces, pointing out the qualitative differences between the various classes and give a compact listing of their characteristic properties. In section 5 we calculate the regularized area for the solution which is of potential use for a map to 4-point scattering amplitudes in s - or t -channel configuration. Section 6 contains a summary and some conclusions. Appendices A and B contain some technical details related to the main text.

¹In physical terms these are vacuum solutions, similar to the four cusp solution in pure AdS_5 . A characterization by invariant geometrical quantities is: intrinsically flat with constant mean curvatures .

2 Space-like strings in $\mathbf{SL}(2, \mathbb{R}) \times \mathbf{SU}(2)$

In this section we describe the $\text{AdS}_3 \times \text{S}^3$ string equations in terms of group variables and integrate these equations in the vacuum sector. We use conformal worldsheet coordinates and gauge fixing conditions, based on a holomorphic structure of space-like string surfaces.

2.1 AdS_3 and S^3 as group manifolds

The AdS_3 and S^3 spaces can be realized as the group manifolds $\text{SL}(2, \mathbb{R})$ and $\text{SU}(2)$ via

$$g = \begin{pmatrix} Y^{0'} + Y^2 & Y^1 + Y^0 \\ Y^1 - Y^0 & Y^{0'} - Y^2 \end{pmatrix}, \quad h = \begin{pmatrix} X^4 + iX^3 & X^2 + iX^1 \\ -X^2 + iX^1 & X^4 - iX^3 \end{pmatrix}. \quad (2.1)$$

Here $Y^K = (Y^{0'}, Y^0, Y^1, Y^2)$ are coordinates of the embedding space $\mathbb{R}^{2,2}$ and the equation for the hyperboloid

$$Y \cdot Y \equiv -Y_{0'}^2 - Y_0^2 + Y_1^2 + Y_2^2 = -1, \quad (2.2)$$

which defines the AdS_3 space, is equivalent to $g \in \text{SL}(2, \mathbb{R})$. Similarly, the equation for S^3 embedded in \mathbb{R}^4

$$X \cdot X \equiv X_1^2 + X_2^2 + X_3^2 + X_4^2 = 1 \quad (2.3)$$

is equivalent to $h \in \text{SU}(2)$.

Let us introduce the following basis in $\mathfrak{sl}(2, \mathbb{R})$

$$\mathbf{t}_0 = \begin{pmatrix} 0 & 1 \\ -1 & 0 \end{pmatrix}, \quad \mathbf{t}_1 = \begin{pmatrix} 0 & 1 \\ 1 & 0 \end{pmatrix}, \quad \mathbf{t}_2 = \begin{pmatrix} 1 & 0 \\ 0 & -1 \end{pmatrix}. \quad (2.4)$$

These three matrices \mathbf{t}_μ ($\mu = 0, 1, 2$) satisfy the relations

$$\mathbf{t}_\mu \mathbf{t}_\nu = \eta_{\mu\nu} \mathbf{I} + \epsilon_{\mu\nu}{}^\rho \mathbf{t}_\rho, \quad (2.5)$$

where $\eta_{\mu\nu} = \text{diag}(-1, 1, 1)$ and $\epsilon_{\mu\nu\rho}$ is the Levi-Civita tensor with $\epsilon_{012} = 1$. The inner product defined by $\langle \mathbf{t}_\mu \mathbf{t}_\nu \rangle \equiv \frac{1}{2} \text{tr}(\mathbf{t}_\mu \mathbf{t}_\nu) = \eta_{\mu\nu}$ provides the isometry between $\mathfrak{sl}(2, \mathbb{R})$ and 3d Minkowski space.

As a basis in $\mathfrak{su}(2)$ we use the anti-hermitian matrices $\mathbf{s}_n = i\boldsymbol{\sigma}_n$ ($n = 1, 2, 3$), where $\boldsymbol{\sigma}_n$ are the Pauli matrices ($\boldsymbol{\sigma}_1 = \mathbf{t}_1$, $\boldsymbol{\sigma}_2 = -i\mathbf{t}_0$, $\boldsymbol{\sigma}_3 = \mathbf{t}_2$). Here one has the algebra

$$\mathbf{s}_m \mathbf{s}_n = -\delta_{mn} \mathbf{I} - \epsilon_{mnl} \mathbf{s}_l, \quad (2.6)$$

and the inner product is introduced by a similarly normalized trace, but with the negative sign $\langle \mathbf{s}_m \mathbf{s}_n \rangle \equiv -\frac{1}{2} \text{tr}(\mathbf{s}_m \mathbf{s}_n) = \delta_{mn}$. That provides the isometry with \mathbb{R}^3 .

Using (2.4), eq. (2.1) can be written as $g = Y^{0'} \mathbf{I} + Y^\mu \mathbf{t}_\mu$, $h = X_4 \mathbf{I} + X_n \mathbf{s}_n$. The inverse group elements respectively become $g^{-1} = Y^{0'} \mathbf{I} - Y^\mu \mathbf{t}_\mu$, $h^{-1} = X_4 \mathbf{I} - X_n \mathbf{s}_n$. With the help of (2.5) and (2.6) one then finds the correspondence between the metric tensors

$$\langle (g^{-1} dg) (g^{-1} dg) \rangle = dY \cdot dY, \quad \langle (h^{-1} dh) (h^{-1} dh) \rangle = dX \cdot dX. \quad (2.7)$$

We use these relations in the next subsection to write the string equations in terms of the group variables.

2.2 String description in terms of group variables

We consider space-like surfaces in $\text{AdS}_3 \times \text{S}^3$. They can be parameterized by conformal complex worldsheet coordinates $z = \frac{1}{2}(\sigma + i\tau)$, $\bar{z} = \frac{1}{2}(\sigma - i\tau)$. In terms of group variables we then get a pair of fields $g(z, \bar{z})$ and $h(z, \bar{z})$, with $g \in \text{SL}(2, \mathbb{R})$ and $h \in \text{SU}(2)$. Using the notation $\partial \equiv \partial_\sigma - i\partial_\tau$, $\bar{\partial} \equiv \partial_\sigma + i\partial_\tau$, the conformal gauge conditions can be written as

$$\langle (g^{-1} \partial g)^2 \rangle + \langle (h^{-1} \partial h)^2 \rangle = 0 = \langle (g^{-1} \bar{\partial} g)^2 \rangle + \langle (h^{-1} \bar{\partial} h)^2 \rangle . \quad (2.8)$$

The string action in this gauge corresponds to the sigma model on $\text{SL}(2, \mathbb{R}) \times \text{SU}(2)$

$$S = \frac{\sqrt{\lambda}}{4\pi} \int d\sigma d\tau [\langle (g^{-1} \partial g) (g^{-1} \bar{\partial} g) \rangle + \langle (h^{-1} \partial h) (h^{-1} \bar{\partial} h) \rangle] , \quad (2.9)$$

where λ is a coupling constant. The variation of (2.9) leads to the equations of motion

$$\partial (g^{-1} \bar{\partial} g) + \bar{\partial} (g^{-1} \partial g) = 0 , \quad \partial (h^{-1} \bar{\partial} h) + \bar{\partial} (h^{-1} \partial h) = 0 . \quad (2.10)$$

From these equations follow the holomorphicity conditions

$$\bar{\partial} \langle (g^{-1} \partial g)^2 \rangle = 0 = \partial \langle (g^{-1} \bar{\partial} g)^2 \rangle , \quad \bar{\partial} \langle (h^{-1} \partial h)^2 \rangle = 0 = \partial \langle (h^{-1} \bar{\partial} h)^2 \rangle , \quad (2.11)$$

for the diagonal components of the induced metric tensors on $\text{SL}(2, \mathbb{R})$ and on $\text{SU}(2)$ separately. These conditions, together with (2.8), allow to use the gauge

$$\langle (g^{-1} \partial g)^2 \rangle = -1 = \langle (g^{-1} \bar{\partial} g)^2 \rangle , \quad \langle (h^{-1} \partial h)^2 \rangle = 1 = \langle (h^{-1} \bar{\partial} h)^2 \rangle . \quad (2.12)$$

The remaining freedom of conformal transformations $z \mapsto f(z)$ in this gauge is given by translations $z \mapsto z + z_0$ and the reflection $z \mapsto -z$. One can also consider $z \mapsto -\bar{z}$, which corresponds to the reflection $\sigma \mapsto -\sigma$.

In the real worldsheet coordinates (σ, τ) the equations of motion (2.10) read

$$\partial_\sigma (g^{-1} \partial_\sigma g) + \partial_\tau (g^{-1} \partial_\tau g) = 0 , \quad \partial_\sigma (h^{-1} \partial_\sigma h) + \partial_\tau (h^{-1} \partial_\tau h) = 0 , \quad (2.13)$$

and the gauge fixing conditions (2.12) are equivalent to

$$\begin{aligned} \langle (g^{-1} \partial_\tau g)^2 \rangle - \langle (g^{-1} \partial_\sigma g)^2 \rangle &= 1 , & \langle (h^{-1} \partial_\sigma h)^2 \rangle - \langle (h^{-1} \partial_\tau h)^2 \rangle &= 1 , \\ \langle (g^{-1} \partial_\sigma g) (g^{-1} \partial_\tau g) \rangle &= 0 , & \langle (h^{-1} \partial_\sigma h) (h^{-1} \partial_\tau h) \rangle &= 0 . \end{aligned} \quad (2.14)$$

The isometry transformations of the group manifolds are given by the left-right multiplications

$$g \mapsto g_L g g_R , \quad h \mapsto h_L h h_R , \quad (2.15)$$

with constant matrices $g_L, g_R \in \text{SL}(2, \mathbb{R})$ and $h_L, h_R \in \text{SU}(2)$. They leave the equations of motion (2.13) and the gauge fixing conditions (2.14) invariant. The system (2.13)-(2.14) is also invariant under the discrete transformations $g \mapsto g^{-1}$ and $h \mapsto h^{-1}$, which correspond to the reflections of Y^0, Y^1, Y^2 and X^1, X^2, X^3 , respectively. Hence, the composition of

$h \mapsto h_L h h_R$ and $h \mapsto h^{-1}$ form the complete group of isometry transformations of $SU(2)$. The complete isometry group of $SL(2, \mathbb{R})$ is obtained as a composition of $g \mapsto g_L g g_R$, $g \mapsto g^{-1}$ and $g \mapsto \mathbf{t}_1 g \mathbf{t}_1$, where the latter corresponds to the reflection of Y^0 and Y^2 .

Using the covariant notation: $(\sigma, \tau) = (\xi^1, \xi^2)$, $\partial_a = \partial_{\xi^a}$ ($a = 1, 2$), the induced metric tensors on the $SL(2, \mathbb{R})$ and $SU(2)$ projections can be written as²

$$f_{ab} = \langle (g^{-1} \partial_a g) (g^{-1} \partial_b g) \rangle, \quad (f_s)_{ab} = \langle (h^{-1} \partial_a h) (h^{-1} \partial_b h) \rangle. \quad (2.16)$$

In the next two subsections we construct solutions corresponding to constant f_{ab} and $(f_s)_{ab}$. First we consider the $SU(2)$ projection, since it is easier to treat. The same method then we apply to the $SL(2, \mathbb{R})$ part.

2.3 Vacuum solutions in $SU(2)$

Let us introduce $\mathfrak{su}(2)$ valued fields related to the right derivatives of h

$$R_\sigma = h^{-1} \partial_\sigma h, \quad R_\tau = h^{-1} \partial_\tau h. \quad (2.17)$$

These fields obey the zero curvature condition

$$\partial_\tau R_\sigma - \partial_\sigma R_\tau = [R_\sigma, R_\tau], \quad (2.18)$$

and the second equation in (2.13) is equivalent to

$$\partial_\sigma R_\sigma + \partial_\tau R_\tau = 0. \quad (2.19)$$

The norms and the scalar product of R_σ and R_τ define the induced metric tensor on the $SU(2)$ projection. We denote the norm of R_τ by ρ_s , and write the $SU(2)$ part of the gauge fixing conditions (2.14) in the form

$$\langle R_\sigma R_\sigma \rangle = 1 + \rho_s^2, \quad \langle R_\tau R_\tau \rangle = \rho_s^2, \quad \langle R_\sigma R_\tau \rangle = 0. \quad (2.20)$$

Our aim is to describe solutions of (2.17)-(2.20) for constant ρ_s . The vectors R_σ , R_τ and $[R_\sigma, R_\tau]$ form an orthogonal basis in $\mathfrak{su}(2)$. Expanding the first derivatives of R_σ and R_τ in this basis, from (2.18)-(2.20) one finds that they have vanishing projections on R_σ and R_τ . Therefore, the first derivatives can be written as³

$$\begin{aligned} \partial_\sigma R_\sigma &= a [R_\sigma, R_\tau], & \partial_\tau R_\sigma &= b [R_\sigma, R_\tau], \\ \partial_\sigma R_\tau &= (b-1) [R_\sigma, R_\tau], & \partial_\tau R_\tau &= -a [R_\sigma, R_\tau]. \end{aligned} \quad (2.21)$$

The consistency conditions of this system are given by the equations

$$\partial_\sigma b = \partial_\tau a, \quad \partial_\tau b = -\partial_\sigma a, \quad a^2 + b^2 - b = 0. \quad (2.22)$$

²In this paper (as in [6]) the index s is used for some variables of the spherical part to distinguish them from similar variables of the AdS part.

³The coefficients on the r.h.s are interpreted as the matrix elements of the second fundamental form.

From the first two equations follows that the coefficients a and b are harmonic functions $a = f_1(z) + \bar{f}_1(\bar{z})$, $b = f_2(z) + \bar{f}_2(\bar{z})$, with $f_2'(z) = i f_1'(z)$. Then, the third equation of (2.22) leads to $f_1'(z) = 0$, which means that a and b are (σ, τ) -independent. Due to the algebraic relation (2.22), the coefficients a and b are parameterized by one angle variable

$$a = \sin \phi_s \cos \phi_s , \quad b = \cos^2 \phi_s , \quad \phi_s \in [0, \pi) . \quad (2.23)$$

As a result, the following linear combination

$$R_0 = \sin \phi_s R_\sigma + \cos \phi_s R_\tau \quad (2.24)$$

is constant.

Now we introduce $\mathfrak{su}(2)$ valued fields with the left derivatives

$$L_\sigma = \partial_\sigma h h^{-1} , \quad L_\tau = \partial_\tau h h^{-1} , \quad (2.25)$$

which are related to the right fields in a standard way

$$L_\sigma = h R_\sigma h^{-1} , \quad L_\tau = h R_\tau h^{-1} . \quad (2.26)$$

The differentiations of (2.26) lead to a system similar to (2.21)

$$\begin{aligned} \partial_\sigma L_\sigma &= a [L_\sigma, L_\tau] , & \partial_\tau L_\sigma &= (b - 1) [L_\sigma, L_\tau] , \\ \partial_\sigma L_\tau &= b [L_\sigma, L_\tau] , & \partial_\tau L_\tau &= -a [L_\sigma, L_\tau] , \end{aligned} \quad (2.27)$$

and one finds that the linear combination

$$L_0 = \cos \phi_s L_\sigma - \sin \phi_s L_\tau \quad (2.28)$$

is also (σ, τ) -independent.

From (2.24) and (2.28) follows that the field h satisfies the equations

$$\frac{\partial h}{\partial l_s} = L_0 h , \quad \frac{\partial h}{\partial r_s} = h R_0 , \quad (2.29)$$

where the new coordinates (l_s, r_s) are related to (σ, τ) by the rotation

$$l_s = \cos \phi_s \sigma - \sin \phi_s \tau , \quad r_s = \sin \phi_s \sigma + \cos \phi_s \tau . \quad (2.30)$$

The integration of the system (2.29) is straightforward and yields

$$h = e^{l_s L_0} h_0 e^{r_s R_0} , \quad (2.31)$$

with an integration constant $h_0 \in \text{SU}(2)$. The isometry transformation $h \mapsto h h_0^{-1}$ brings the solution to the form $h = e^{l_s L_0} e^{r_s R_1}$, with $R_1 = h_0 R_0 h_0^{-1}$. Denoting L_0 by L_s and R_1 by R_s , we obtain

$$h = e^{l_s L_s} e^{r_s R_s} . \quad (2.32)$$

This field indeed solves equation (2.19) for any pair of constant vectors L_s and R_s .

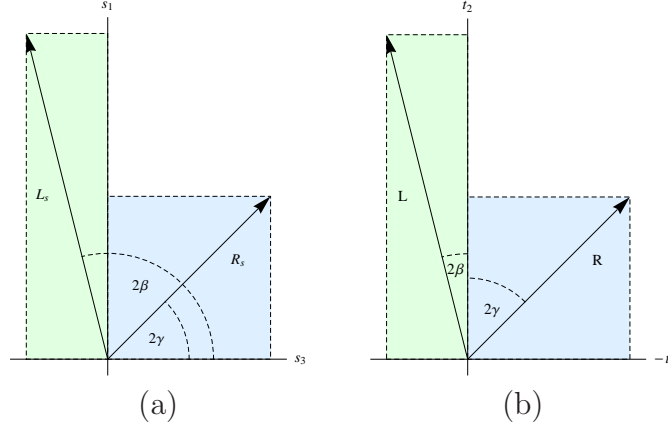


Figure 1: The pair (L_s, R_s) in the first plot is identified with two vectors in \mathbb{R}^3 located in the plane $(3, 1)$. Similarly, L and R in the second plot are 3d Minkowski vectors with vanishing time components.

To verify the orthonormality conditions (2.20) we calculate the induced metric tensor in the coordinates (l_s, r_s) . From (2.32) follows its matrix form

$$(f_s)_{ab}(l_s, r_s) = \begin{pmatrix} \langle L_s L_s \rangle & \langle L_s R_s \rangle \\ \langle L_s R_s \rangle & \langle R_s R_s \rangle \end{pmatrix}. \quad (2.33)$$

On the other hand, the map (2.30) defines the same tensor as

$$M \begin{pmatrix} 1 + \rho_s^2 & 0 \\ 0 & \rho_s^2 \end{pmatrix} M^T = \begin{pmatrix} \rho_s^2 + \cos^2 \phi_s & \sin \phi_s \cos \phi_s \\ \sin \phi_s \cos \phi_s & \rho_s^2 + \sin^2 \phi_s \end{pmatrix}, \quad (2.34)$$

where M is the rotation matrix in (2.30). Comparing (2.33) and (2.34), one finds

$$\langle L_s L_s \rangle = \rho_s^2 + \cos^2 \phi_s, \quad \langle R_s R_s \rangle = \rho_s^2 + \sin^2 \phi_s, \quad \langle L_s R_s \rangle = \sin \phi_s \cos \phi_s. \quad (2.35)$$

The obtained norms of L_s and R_s are consistent with (2.28) and (2.24). A new result from this calculation is the scalar product $\langle L_s R_s \rangle$, which defines the angle between these vectors.

Now we describe how to factorize the left-right symmetry (2.15) and parameterize the $SU_L(2) \otimes SU_R(2)$ orbits of solutions by the pairs (ρ_s, ϕ_s) .

Since the general case (2.31) reduces to (2.32) by right (or left) multiplications, it is enough to classify the fields (2.32). This factorized form of solutions is invariant under the similarity transformations $h \mapsto h_L h h_L^{-1}$, which rotate the vectors L_s and R_s by the adjoint representation: $L_s \mapsto h_L L_s h_L^{-1}$, $R_s \mapsto h_L R_s h_L^{-1}$. The adjoint representation is equivalent to $SO(3)$ and it is convenient to interpret L_s and R_s as vectors in \mathbb{R}^3 . Using this picture, one can easily bring any pair (L_s, R_s) to some canonical form defined only by the scalar invariants (2.35). Note that the commutator $[L_s, R_s]$ transforms also by the adjoint representation, its norm is given by $\langle [L_s, R_s]^2 \rangle = 4\rho_s^2(1 + \rho_s^2)$ and one can use this vector to specify a canonical pair (L_s, R_s) . We choose the pair

$$L_s = -\rho_s \sin \phi_s \mathbf{s}_3 + \sqrt{1 + \rho_s^2} \cos \phi_s \mathbf{s}_1, \quad R_s = \rho_s \cos \phi_s \mathbf{s}_3 + \sqrt{1 + \rho_s^2} \sin \phi_s \mathbf{s}_1. \quad (2.36)$$

It corresponds to

$$[L_s, R_s] = 2\rho_s \sqrt{1 + \rho_s^2} \mathbf{s}_2, \quad (2.37)$$

and, in addition, the vectors L_s and R_s are oriented in some symmetric way in the $(\mathbf{s}_3, \mathbf{s}_1)$ plane. Namely, the two rectangles formed by the components of the vectors L_s and R_s have the same area (see fig. 1(a)). The choice (2.36) is motivated by its relevance for the generalization to the $SL(2, \mathbb{R})$ case. It is also helpful to establish contact with Pohlmeyer reduction.

The calculation of the exponents $e^{l_s L_s}$ and $e^{r_s R_s}$ corresponding to (2.36) is straightforward. However, in general, the solution (2.32) has a rather complicated matrix form. One can simplify it by an isometry transformation. For this purpose we rewrite (2.36) as

$$L_s = |L_s| e^{-i\beta \sigma_2} \mathbf{s}_3 e^{i\beta \sigma_2}, \quad R_s = |R_s| e^{-i\gamma \sigma_2} \mathbf{s}_3 e^{i\gamma \sigma_2}, \quad (2.38)$$

where $(|L_s|, 2\beta)$ and $(|R_s|, 2\gamma)$ are the polar coordinates in the $(\mathbf{s}_3, \mathbf{s}_1)$ plane for the vectors L_s and R_s , respectively (see fig. 1(a)). Using then (A.4) and multiplying the solution (2.32) by $e^{i\beta \sigma_2}$ from the l.h.s and by $e^{-i\gamma \sigma_2}$ from the r.h.s., we obtain the new solution

$$h = e^{i\tilde{l}_s \sigma_3} e^{i\theta_s \sigma_2} e^{i\tilde{r}_s \sigma_3} = \begin{pmatrix} \cos \theta_s e^{i\xi_s} & \sin \theta_s e^{i\eta_s} \\ -\sin \theta_s e^{-i\eta_s} & \cos \theta_s e^{-i\xi_s} \end{pmatrix}. \quad (2.39)$$

Here \tilde{l}_s and \tilde{r}_s are the rescaled worldsheet coordinates

$$\tilde{l}_s = |L_s| l_s, \quad \tilde{r}_s = |R_s| r_s, \quad (2.40)$$

$\xi_s = \tilde{l}_s + \tilde{r}_s$, $\eta_s = \tilde{l}_s - \tilde{r}_s$ and $2\theta_s = 2\beta - 2\gamma$ corresponds to the angle between L_s and R_s

$$\cos 2\theta_s = \frac{\langle L_s R_s \rangle}{|L_s| |R_s|}, \quad 2\theta_s \in (0, \pi). \quad (2.41)$$

By (2.35) one has

$$\cot 2\theta_s = \frac{\sin \phi_s \cos \phi_s}{\rho_s \sqrt{1 + \rho_s^2}}. \quad (2.42)$$

The embedding coordinates for the solution (2.39) are given by

$$X_1 = \sin \theta_s \sin \eta_s, \quad X_2 = \sin \theta_s \cos \eta_s, \quad X_3 = \cos \theta_s \sin \xi_s, \quad X_4 = \cos \theta_s \cos \xi_s. \quad (2.43)$$

The pairs (X_1, X_2) and (X_3, X_4) here are on the circles

$$X_1^2 + X_2^2 = \sin^2 \theta_s, \quad X_3^2 + X_4^2 = \cos^2 \theta_s. \quad (2.44)$$

Therefore, eq. (2.43) describes a torus in $S^3 \subset \mathbb{R}^4$ with the radii $\sin \theta_s$ and $\cos \theta_s$.

The solution (2.43) was obtained in [6] via Pohlmeyer reduction. It was shown that the mean curvature of the embedding in S^3 is equal to

$$H_s = \cot 2\theta_s. \quad (2.45)$$

From (2.32) follows the equation

$$\langle L_s h R_s h^{-1} \rangle = \langle L_s R_s \rangle , \quad (2.46)$$

which defines a surface in $SU(2)$ in a form independent of worldsheet coordinates. Since h and h^{-1} are linear functions of the embedding coordinates, the l.h.s. of (2.46) provides a quadric in these variables. The corresponding surface expressed in \mathbb{R}^4 embedding coordinates is given as an intersection of the $S^3 \subset \mathbb{R}^4$ and

$$X_4^2 \langle L_s R_s \rangle + X_4 X_n \langle L_s [s_n, R_s] \rangle - X_n X_m \langle L_s s_m R_s s_n \rangle = \langle L_s R_s \rangle . \quad (2.47)$$

Taking L_s and R_s from (2.38), after simple transformations one can rewrite (2.46) in the form

$$\langle \mathbf{s}_3 h \mathbf{s}_3 h^{-1} \rangle = \cos 2\theta_s , \quad (2.48)$$

which reproduces (2.44). Though this surface in $SU(2)$ is described only by θ_s , this parameter is not a complete characteristic of the $SU(2)$ part for our system in $SL(2, \mathbb{R}) \times SU(2)$. Since we are in a fixed gauge, ρ_s also has a certain gauge invariant meaning. Namely, $\rho_s \sqrt{1 + \rho_s^2} d\sigma d\tau$ defines the area measure on the surface induced from S^3 .

Finally, note that L_s and R_s are related to the Noether integrals of the isometry group and therefore they have also a gauge invariant meaning.

2.4 Vacuum solutions in $SL(2, \mathbb{R})$

Based on the isometry between the $\mathfrak{sl}(2, \mathbb{R})$ algebra and 3d Minkowski space, we call a vector $\mathbf{a} \in \mathfrak{sl}(2, \mathbb{R})$ space-like if $\langle \mathbf{a} \mathbf{a} \rangle > 0$, time-like if $\langle \mathbf{a} \mathbf{a} \rangle < 0$ and light-like if $\langle \mathbf{a} \mathbf{a} \rangle = 0$.

Note that the vector $g^{-1} \partial_\tau g$ is space-like in the gauge (2.14). Similarly to the $SU(2)$ case, we introduce the notation $\rho^2 \equiv \langle (g^{-1} \partial_\tau g)^2 \rangle$ and write the induced metric tensor on the $SL(2, \mathbb{R})$ projection in the form⁴

$$f_{ab}(\sigma, \tau) = \begin{pmatrix} \rho^2 - 1 & 0 \\ 0 & \rho^2 \end{pmatrix} . \quad (2.49)$$

The sum with the $SU(2)$ metric (2.20) gives the total metric induced from $SL(2, \mathbb{R}) \times SU(2)$ and is by construction a multiple of the identity matrix. The metric (2.49) is space-like if $\rho^2 > 1$, it is time-like if $0 < \rho^2 < 1$ and it becomes light-like if $\rho^2 = 1$. The last case corresponds to a degenerate metric with a light-like vector $g^{-1} \partial_\sigma g$.

We consider constant ρ^2 and apply the scheme of the previous subsection. The case of light-like R_σ is special and we consider it separately. If R_σ is space-like or time-like, the vectors R_σ , R_τ and $[R_\sigma, R_\tau]$ form an orthonormal basis in $\mathfrak{sl}(2, \mathbb{R})$. Repeating then the same steps as in $SU(2)$ we come to the factorized type solution (2.32)

$$g = e^{L L} e^{R R} . \quad (2.50)$$

⁴This form differs from the one used in [6]. There the $(\tau\tau)$ -component of the induced metric tensor was denoted by $1 + \rho^2$ for the space-like surfaces and by $1 - \rho^2$ for the time-like ones. Note also, that in our convention σ is time-like in the time-like case.

Here (L, R) is a pair of constant elements of the $\mathfrak{sl}(2, \mathbb{R})$ algebra and (l, r) are worldsheet coordinates obtained from (σ, τ) by a rotation on an angle ϕ which parameterizes the coefficients of the linear system (see (2.21))

$$a = \frac{\langle \partial_\sigma R_\sigma [R_\sigma, R_\tau] \rangle}{\langle [R_\sigma, R_\tau]^2 \rangle}, \quad b = \frac{\langle \partial_\tau R_\sigma [R_\sigma, R_\tau] \rangle}{\langle [R_\sigma, R_\tau]^2 \rangle}. \quad (2.51)$$

Now $R_\sigma = g^{-1} \partial_\sigma g$, $R_\tau = g^{-1} \partial_\tau g$ and a, b satisfy again (2.22). For further convenience, we use here a different parameterization

$$a = -\sin \phi \cos \phi, \quad b = \sin^2 \phi, \quad \phi \in (-\pi/2, \pi/2], \quad (2.52)$$

which is obtained from (2.23) by the replacements $\cos \phi_s \mapsto \sin \phi$, $\sin \phi_s \mapsto -\cos \phi$. This provides the following (l, r) coordinates (compare with (2.30))

$$l = \cos \phi \tau + \sin \phi \sigma, \quad r = \sin \phi \tau - \cos \phi \sigma. \quad (2.53)$$

If R_σ is light-like, one gets the commutator⁵

$$[R_\sigma, R_\tau] = 2 R_\sigma. \quad (2.54)$$

Hence, in this case, R_σ, R_τ and $[R_\sigma, R_\tau]$ do not form a basis in $\mathfrak{sl}(2, \mathbb{R})$. Completing R_σ and R_τ in a suitable way to a basis, one can show that in the end the third independent direction is not needed to express the derivatives of R_σ and R_τ . For details see the parallel discussion of this issue in the framework of Pohlmeyer reduction in section 3.3 below. Altogether the system (2.21) is modified and replaced by the linear system

$$\begin{aligned} \partial_\sigma R_\sigma &= 2a R_\sigma, & \partial_\tau R_\sigma &= 2b R_\sigma, \\ \partial_\sigma R_\tau &= 2(b-1) R_\sigma, & \partial_\tau R_\tau &= -2a R_\sigma. \end{aligned} \quad (2.55)$$

The consistency conditions for this system lead to the equations

$$\partial_\tau a - \partial_\sigma b = 0, \quad \partial_\sigma a + \partial_\tau b + 2(a^2 + b^2 - b) = 0, \quad (2.56)$$

which, in contrast to other cases, do not necessarily require constant a and b . In section 3.3 we describe also the general solution of the consistency conditions (2.56) and indicate how to integrate the linear system (2.55). Here we identify vacuum configurations with the solutions for constant a and b . In this case (2.56) reduces again to $a^2 + b^2 - b = 0$ and one can use the parameterization (2.52). Constant currents (L, R) are then constructed in a same way and one again obtains solutions in the factorized form (2.50). Thus, (2.50) represents solutions in the vacuum sector for all three cases: $\rho^2 > 1$, $\rho^2 < 1$ and $\rho^2 = 1$ as well.

The induced metric tensor in (l, r) -coordinates, calculated by (2.49) and (2.53), becomes

$$f_{ab}(l, r) = \begin{pmatrix} \rho^2 - \sin^2 \phi & \sin \phi \cos \phi \\ \sin \phi \cos \phi & \rho^2 - \cos^2 \phi \end{pmatrix}, \quad (2.57)$$

⁵Note that (2.54) is equivalent to $[(\mathbf{t}_1 - \mathbf{t}_0), \mathbf{t}_2] = 2(\mathbf{t}_1 - \mathbf{t}_0)$.

and comparing it with the calculation from (2.50), one finds

$$\langle LL \rangle = \rho^2 - \sin^2 \phi, \quad \langle RR \rangle = \rho^2 - \cos^2 \phi, \quad \langle LR \rangle = \sin \phi \cos \phi. \quad (2.58)$$

These equations fix the norm of the commutator $[L, R]$ to

$$\langle [L, R]^2 \rangle = 4\rho^2(1 - \rho^2). \quad (2.59)$$

Thus, $[L, R]$ is time-like for space-like surfaces ($\rho^2 > 1$), $[L, R]$ is light-like for light-like surfaces ($\rho^2 = 1$) and $[L, R]$ is space-like for time-like surfaces ($\rho^2 < 0$).

We use these metric characteristics of the commutator $[L, R]$ and also the scalars (2.58) to classify the fields g by the adjoint orbits similarly to the previous subsection. Since the adjoint representation of $\text{SL}(2, \mathbb{R})$ is given by the group of proper Lorentz transformations $\text{SO}_\uparrow(1, 2)$, the orbits can be identified with the hyperbolas and cones in 3d Minkowski space. Choosing canonical pairs (L, R) from the orbits, one can construct solutions by (2.50) and then simplify them as in (2.39). This procedure also simplifies the form of the quadratic relation between the $\mathbb{R}^{2,2}$ embedding coordinates, which is now given by

$$\langle LgRg^{-1} \rangle = (Y^{0'})^2 \langle LR \rangle + Y^\mu Y^{0'} \langle L[t_\mu, R] \rangle - Y^\mu Y^\nu \langle Lt_\mu Rt_\nu \rangle = \langle LR \rangle. \quad (2.60)$$

It is natural to divide the solutions in three classes according to the signature of the induced metric tensor and then continue classification inside the classes.

Before starting classification it is useful to note that the reflection freedom $\sigma \mapsto -\sigma$ allows to set $a \leq 0$ (see eqs. (2.51)-(2.52) and (2.55)). This corresponds to $\phi \in [0, \pi/2]$. Below we assume this condition.

1. Space-like surfaces ($\rho^2 > 1$).

This case corresponds to space-like L, R and time-like $[L, R]$. One can take the commutator $[L, R]$ proportional to \mathbf{t}_0 . However, in contrast to the $\text{SU}(2)$ case there are two possibilities

$$[L, R] = \pm 2\rho\sqrt{\rho^2 - 1} \mathbf{t}_0, \quad (2.61)$$

which are not on the same adjoint orbit. These two cases are related by the discrete isometry transformation $g \mapsto \mathbf{t}_1 g \mathbf{t}_1$.

Let us consider the negative sign in (2.61) and choose the pair

$$L = \rho \cos \phi \mathbf{t}_2 + \sqrt{\rho^2 - 1} \sin \phi \mathbf{t}_1, \quad R = \rho \sin \phi \mathbf{t}_2 - \sqrt{\rho^2 - 1} \cos \phi \mathbf{t}_1. \quad (2.62)$$

Using the same trick as in (2.38), based now on (A.7), we first rewrite (2.62) in the form

$$L = |L| e^{-\beta \mathbf{t}_0} \mathbf{t}_2 e^{\beta \mathbf{t}_0}, \quad R = |R| e^{-\gamma \mathbf{t}_0} \mathbf{t}_2 e^{\gamma \mathbf{t}_0}, \quad (2.63)$$

where $|L| = \sqrt{\rho^2 - \sin^2 \phi}$, $|R| = \sqrt{\rho^2 - \cos^2 \phi}$, and $(2\beta, 2\gamma)$ are the polar angles in the $(\mathbf{t}_2, \mathbf{t}_1)$ plane, (see fig. 1(b)). Then, as in (2.39), the left-right multiplications reduce the solution (2.50) to

$$g = e^{\tilde{l} \mathbf{t}_2} e^{\theta \mathbf{t}_0} e^{\tilde{r} \mathbf{t}_2} = \begin{pmatrix} \cos \theta e^\xi & \sin \theta e^\eta \\ -\sin \theta e^{-\eta} & \cos \theta e^{-\xi} \end{pmatrix}. \quad (2.64)$$

Here $\tilde{l} = |L|l$ and $\tilde{r} = |R|r$ are the rescaled worldsheet coordinates, $\xi = \tilde{l} + \tilde{r}$, $\eta = \tilde{l} - \tilde{r}$ and $2\theta = 2\beta - 2\gamma$ is the angle between the vectors (2.62), with

$$\cot 2\theta = \frac{\sin \phi \cos \phi}{\rho \sqrt{\rho^2 - 1}}, \quad \theta \in (0, \pi/4]. \quad (2.65)$$

The embedding coordinates for the solution (2.64) are given by

$$Y^{0'} = \cos \theta \cosh \xi, \quad Y^0 = \sin \theta \cosh \eta, \quad Y^1 = \sin \theta \sinh \eta, \quad Y^2 = \cos \theta \sinh \xi. \quad (2.66)$$

This surface was also obtained in [6] by Pohlmeyer reduction. Its mean curvature is

$$H = \cot 2\theta. \quad (2.67)$$

Similarly to (2.48), the quadric (2.60) reduces to

$$(Y^0)^2 - (Y^1)^2 = \sin^2 \theta, \quad (2.68)$$

and for $\theta = \pi/4$ it reproduces the four cusp surface of [3, 1].

Like in (2.43), the shape of the surface (2.66) depends only on the parameter θ , and not on ρ and ϕ separately. The first plot in fig. 2 shows the constant θ lines on the strip with the coordinates $(\sin^2 \phi, \rho^2)$. From (2.65) follows that these lines are arcs of ellipses for the space-like surfaces ($\rho^2 > 1$). One can check (see below the analog of (2.65)) that the lines become arcs of hyperbolas for $\rho^2 < 1$. The second plot in fig. 2 is used for a classification of the surfaces which we consider below. Note again that different points on the constant θ lines describe different solutions of the system in $\text{AdS}_3 \times S^3$, though they have the same AdS_3 projection.

In fig. 3 we present the surfaces in AdS_3 associated with different solutions of our system. The surface (2.66) is shown in the plot 3(a).

2. Light-like surfaces ($\rho^2 = 1$).

The commutator $[L, R]$ is light-like for $\rho^2 = 1$ and one has again two options

$$[L, R] = \pm 2\mathbf{t}_+ \equiv \pm(\mathbf{t}_0 + \mathbf{t}_1), \quad (2.69)$$

which are not on the same adjoint orbit. The option $[L, R] = -2\mathbf{t}_+$ can be realized by

$$L = \cos \phi \mathbf{t}_2 + \sin \phi \mathbf{t}_+, \quad R = \sin \phi \mathbf{t}_2 - \cos \phi \mathbf{t}_+. \quad (2.70)$$

Note that the pair $(-L, -R)$ has the same commutator and the scalar invariants (2.58) as (L, R) . However, these two pairs are on different adjoint orbits. We have the same situation for $[L, R] = 2\mathbf{t}_+$. Hence, for $\rho^2 = 1$, there are four sets of adjoint orbits of (L, R) pairs. They are related to each other by discrete isometry transformations. Therefore, it is sufficient to consider only (2.70). It splits into three subcases:

- 2.1) $\phi = 0$; 2.2) $\phi = \pi/2$; 2.3) $\phi \in (0, \pi/2)$.

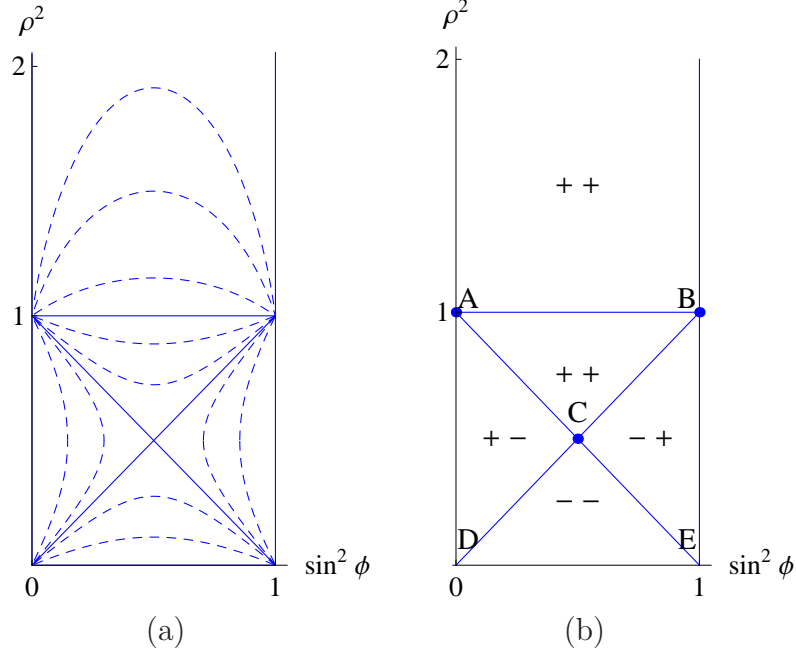


Figure 2: The dashed lines in the first plot correspond to constant θ . The left and right signs in the second plot correspond to the signs of $\langle L^2 \rangle$ and $\langle R^2 \rangle$, respectively. $\langle L^2 \rangle$ vanishes at the diagonal BD and $\langle R^2 \rangle$ at AE .

Case 2.1. $\phi = 0$ corresponds to the point A in fig. 2(b).

Now $\langle LL \rangle = 1$, $\langle RR \rangle = 0$, $\langle LR \rangle = 0$; $l = \tau$, $r = -\sigma$. Then, eq. (2.50) yields the solution

$$g = e^{\tau t_2} e^{\sigma t_+} = \begin{pmatrix} e^\tau & \sigma e^\tau \\ 0 & e^{-\tau} \end{pmatrix}, \quad (2.71)$$

with the embedding coordinates

$$Y^{0'} = \cosh \tau, \quad Y^0 = \frac{\sigma}{2} e^\tau, \quad Y^1 = \frac{\sigma}{2} e^\tau, \quad Y^2 = \sinh \tau. \quad (2.72)$$

The quadric (2.60) here reduces to

$$(Y^0 - Y^1)(Y^{0'} + Y^2) = 0, \quad (2.73)$$

which is realized by (2.72) in the linear form $Y^0 - Y^1 = 0$. The surface (2.72) is given by the plot 3(b). It has two cusps at the boundary.

Case 2.2. $\phi = \pi/2$ corresponds to the point B in fig. 2(b).

Here $\langle LL \rangle = 0$, $\langle RR \rangle = 1$, $\langle LR \rangle = 0$; $l = \sigma$, $r = \tau$. The solution (2.50) now becomes

$$g = e^{\sigma t_+} e^{\tau t_2} = \begin{pmatrix} e^\tau & \sigma e^{-\tau} \\ 0 & e^{-\tau} \end{pmatrix}, \quad (2.74)$$

with the embedding coordinates

$$Y^{0'} = \cosh \tau, \quad Y^0 = \frac{\sigma}{2} e^{-\tau}, \quad Y^1 = \frac{\sigma}{2} e^{-\tau}, \quad Y^2 = \sinh \tau, \quad (2.75)$$

and the quadric $(Y^0 - Y^1)(Y^{0'} - Y^2) = 0$. This surface is obtained from (2.73) by the reflection $Y^2 \mapsto -Y^2$. Hence, the plot 3(b) represents (2.75) as well.

Case 2.3. $\phi \in (0, \pi/2)$ corresponds to the segment between the points A and B in fig. 2(b).

In this case $\langle LL \rangle = \cos^2 \phi > 0$, $\langle RR \rangle = \sin^2 \phi > 0$. Here we simplify the solution (2.50) by the same trick as in (2.38)-(2.39). Using (A.8), we write (2.70) as

$$L = \cos \phi e^{-\beta \mathbf{t}_+} \mathbf{t}_2 e^{\beta \mathbf{t}_+}, \quad R = \sin \phi e^{-\gamma \mathbf{t}_+} \mathbf{t}_2 e^{\gamma \mathbf{t}_+}, \quad (2.76)$$

and bring the solution (2.50) to the form $e^{l \cos \phi \mathbf{t}_2} e^{\theta \mathbf{t}_+} e^{r \sin \phi \mathbf{t}_2}$, with $\theta = \beta - \gamma = 1/\sin 2\phi$. By the rescaling property $e^{\lambda \mathbf{t}_2} \mathbf{t}_+ e^{-\lambda \mathbf{t}_2} = e^{2\lambda} \mathbf{t}_+$, we then set $\theta = 1$ and get

$$g = e^{l \cos \phi \mathbf{t}_2} e^{\mathbf{t}_+} e^{r \sin \phi \mathbf{t}_2} = \begin{pmatrix} e^\tau & e^{\tilde{\tau}} \\ 0 & e^{-\tau} \end{pmatrix}, \quad \tilde{\tau} = \tau \cos 2\phi + \sigma \sin 2\phi. \quad (2.77)$$

This solution satisfies the relation $\langle \mathbf{t}_2 g \mathbf{t}_2 g^{-1} \rangle = 1$, which reduces to

$$(Y^0)^2 - (Y^1)^2 = 0, \quad (2.78)$$

and it can be treated as a limiting case of (2.68) at $\theta \rightarrow 0$. The embedding coordinates

$$Y^{0'} = \cosh \tau, \quad Y^0 = \frac{e^{\tilde{\tau}}}{2}, \quad Y^1 = \frac{e^{\tilde{\tau}}}{2}, \quad Y^2 = \sinh \tau \quad (2.79)$$

realize (2.78) by $Y^0 - Y^1 = 0$ as in (2.72). The difference with the case 2.1 is that now Y^0 and Y^1 are positive on the worldsheet. This surface is given by the plot 3(c) and has one cusp at the boundary. The line crossing the interior of AdS_3 corresponds to $\tilde{\tau} \rightarrow -\infty$. Although now the projection to AdS_3 has a boundary inside AdS_3 , the surface itself has there no boundary inside $\text{AdS}_3 \times S^3$, since $\tilde{\tau} \rightarrow -\infty$ is correlated with infinitely wrapping the torus in S^3 .

Concluding this part we note that the calculation of (2.50) for L and R given by (2.70) leads to the answer

$$g = e^{lL} e^{rR} = \begin{pmatrix} e^\tau & \mu \\ 0 & e^{-\tau} \end{pmatrix}, \quad \mu = \frac{e^{\tilde{\tau}} - \cosh \tau - \cos 2\phi \sinh \tau}{\sin 2\phi}. \quad (2.80)$$

The isometry transformations described above simplify its g_{12} component to (2.77).

The solution (2.80) provides the following embedding coordinates

$$Y^{0'} = \cosh \tau, \quad Y^0 = \frac{e^{\tilde{\tau}} - \cosh \tau - \cos 2\phi \sinh \tau}{2 \sin 2\phi} = Y^1, \quad Y^2 = \sinh \tau, \quad (2.81)$$

which in the limit $\phi \rightarrow 0$ and $\phi \rightarrow \pi/2$ reproduces (2.72) and (2.75), respectively.

3. Time-like surfaces ($\rho^2 < 1$).

Here $[L, R]$ is space-like and we can fix it by

$$[L, R] = -2\rho\sqrt{1 - \rho^2} \mathbf{t}_1. \quad (2.82)$$

L and R are then in the plane $(\mathbf{t}_2, \mathbf{t}_0)$ and the pairs (L, R) and $(-L, -R)$ belong to different adjoint orbits, generated by \mathbf{t}_1 . Hence, there are two options for (L, R) , which are related to each other through the discrete isometry transformation $g \mapsto \mathbf{t}_1 g \mathbf{t}_1$.

Similarly to (2.62), we choose the pair

$$L = \rho \cos \phi \mathbf{t}_2 + \sqrt{1 - \rho^2} \sin \phi \mathbf{t}_0, \quad R = \rho \sin \phi \mathbf{t}_2 - \sqrt{1 - \rho^2} \cos \phi \mathbf{t}_0, \quad (2.83)$$

which now allows all three possibilities (space-like, light-like, time-like) for both L and R . The corresponding nine cases are represented in fig. 2(b) inside the square $\rho^2 < 1$ and we enumerate them in the following order:

Case 3.1 $\langle LL \rangle > 0, \langle RR \rangle > 0$.

This corresponds to the area inside the triangle ABC in fig. 2(b).

Here $\rho^2 > \max[\sin^2 \phi, \cos^2 \phi]$, which implies $\rho \sqrt{1 - \rho^2} < \sin \phi \cos \phi$ and $\rho^2 > 1/2$.

The space-like vectors (2.83) can be written in the form (2.38)

$$L = \sqrt{\rho^2 - \sin^2 \phi} e^{-\beta \mathbf{t}_1} \mathbf{t}_2 e^{\beta \mathbf{t}_1}, \quad R = \sqrt{\rho^2 - \cos^2 \phi} e^{-\gamma \mathbf{t}_1} \mathbf{t}_2 e^{\gamma \mathbf{t}_1}, \quad (2.84)$$

using the boost parameters β and γ . Applying then the same trick as above, we find the solution

$$g = e^{\tilde{l} \mathbf{t}_2} e^{\theta \mathbf{t}_1} e^{\tilde{r} \mathbf{t}_2} = \begin{pmatrix} \cosh \theta e^\xi & \sinh \theta e^\eta \\ \sinh \theta e^{-\eta} & \cosh \theta e^{-\xi} \end{pmatrix}, \quad (2.85)$$

where

$$\tilde{l} = \sqrt{\rho^2 - \sin^2 \phi} l, \quad \tilde{r} = \sqrt{\rho^2 - \cos^2 \phi} r \quad (2.86)$$

are the rescaled coordinates, $\xi = \tilde{l} + \tilde{r}$, $\eta = \tilde{l} - \tilde{r}$, and the new boost parameter $\theta = \beta - \gamma > 0$ is given by

$$\tanh 2\theta = \frac{\rho \sqrt{1 - \rho^2}}{\sin \phi \cos \phi}. \quad (2.87)$$

The embedding coordinates

$$Y^{0'} = \cosh \theta \cosh \xi, \quad Y^0 = \sinh \theta \sinh \eta, \quad Y^1 = \sinh \theta \cosh \eta, \quad Y^2 = \cosh \theta \sinh \xi \quad (2.88)$$

satisfy the quadric

$$(Y^1)^2 - (Y^0)^2 = \sinh^2 \theta. \quad (2.89)$$

The solution (2.88) was obtained in [6] by an analytical continuation of the space-like case (2.66). The corresponding surface is shown in the plot 3(d). It also has four cusps, however, now only two of them are separated by a space-like interval and the other two by a time-like one.

Case 3.2 $\langle LL \rangle > 0, \langle RR \rangle = 0$.

This corresponds to the open line segment between the points A and C in fig. 2(b).

Here $\rho^2 = \cos^2 \phi > \sin^2 \phi$, i.e. $\sin \phi = \sqrt{1 - \rho^2}$, $\phi \in (0, \pi/4)$ and $\rho^2 > 1/2$.

The pair (2.83) now takes the form

$$L = \rho^2 \mathbf{t}_2 + (1 - \rho^2) \mathbf{t}_0, \quad R = \rho \sqrt{1 - \rho^2} (\mathbf{t}_2 - \mathbf{t}_0), \quad (2.90)$$

and one gets $L = \sqrt{2\rho^2 - 1} e^{-\beta \mathbf{t}_1} \mathbf{t}_2 e^{\beta \mathbf{t}_1}$, with $e^{2\beta} = (2\rho^2 - 1)^{-\frac{1}{2}}$. Using then the identity $e^{\beta \mathbf{t}_1} (\mathbf{t}_2 - \mathbf{t}_0) e^{-\beta \mathbf{t}_1} = e^{2\beta} (\mathbf{t}_2 - \mathbf{t}_0)$, and the multiplication trick, we obtain the solution

$$g = e^{\tilde{l} \mathbf{t}_2} e^{\tilde{r} (\mathbf{t}_2 - \mathbf{t}_0)} = \begin{pmatrix} e^{\tilde{l}} (1 + \tilde{r}) & -e^{\tilde{l}} \tilde{r} \\ e^{-\tilde{l}} \tilde{r} & e^{-\tilde{l}} (1 - \tilde{r}) \end{pmatrix}, \quad (2.91)$$

where \tilde{l} and \tilde{r} are the rescaled worldsheet coordinates

$$\tilde{l} = \sqrt{2\rho^2 - 1} l, \quad \tilde{r} = \frac{\rho \sqrt{1 - \rho^2}}{\sqrt{2\rho^2 - 1}} r. \quad (2.92)$$

The embedding coordinates for (2.91)

$$Y^{0'} = \cosh \tilde{l} + \tilde{r} \sinh \tilde{l}, \quad Y^0 = -\tilde{r} \cosh \tilde{l}, \quad Y^1 = -\tilde{r} \sinh \tilde{l}, \quad Y^2 = \tilde{r} \cosh \tilde{l} + \sinh \tilde{l}, \quad (2.93)$$

satisfy the quadric

$$(Y^{0'} + Y^1)^2 - (Y^0 + Y^2)^2 = 1. \quad (2.94)$$

This surface is depicted in the plot 3(e). It has again four cusps at the boundary, but the separation of the opposite points at the diagonals are different than the one in the previous cases. We analyze the boundary behavior of the surfaces in section 4.

Case 3.3 $\langle LL \rangle > 0$, $\langle RR \rangle < 0$.

This corresponds to the area inside the triangle ACD in fig. 2(b).

Here $\sin^2 \phi < \rho^2 < \cos^2 \phi$, i.e. $\sin \phi \cos \phi < \rho \sqrt{1 - \rho^2}$, and one writes the pair (2.83) as

$$L = \sqrt{\rho^2 - \sin^2 \phi} e^{-\beta \mathbf{t}_1} \mathbf{t}_2 e^{\beta \mathbf{t}_1}, \quad R = -\sqrt{\cos^2 \phi - \rho^2} e^{-\gamma \mathbf{t}_1} \mathbf{t}_0 e^{\gamma \mathbf{t}_1}, \quad (2.95)$$

with the boost parameters β and γ . Then, similarly to (2.85), we find the solution

$$g = e^{\tilde{l} \mathbf{t}_2} e^{\theta \mathbf{t}_1} e^{-\tilde{r} \mathbf{t}_0} = \begin{pmatrix} \cosh \theta e^{\tilde{l}} \cos \tilde{r} + \sinh \theta e^{\tilde{l}} \sin \tilde{r} & \sinh \theta e^{\tilde{l}} \cos \tilde{r} - \cosh \theta e^{\tilde{l}} \sin \tilde{r} \\ \sinh \theta e^{-\tilde{l}} \cos \tilde{r} + \cosh \theta e^{-\tilde{l}} \sin \tilde{r} & \cosh \theta e^{-\tilde{l}} \cos \tilde{r} - \sinh \theta e^{-\tilde{l}} \sin \tilde{r} \end{pmatrix}, \quad (2.96)$$

where the rescaled coordinates are $\tilde{l} = \sqrt{\rho^2 - \sin^2 \phi} l$, $\tilde{r} = \sqrt{\cos^2 \phi - \rho^2} r$, and the new boost parameter $\theta = \beta - \gamma > 0$ is given by

$$\tanh 2\theta = \frac{\sin \phi \cos \phi}{\rho \sqrt{1 - \rho^2}}. \quad (2.97)$$

The embedding coordinates in this case

$$\begin{aligned} Y^{0'} &= \cosh \theta \cosh \tilde{l} \cos \tilde{r} + \sinh \theta \sinh \tilde{l} \sin \tilde{r}, & Y^0 &= \sinh \theta \sinh \tilde{l} \cos \tilde{r} - \cosh \theta \cosh \tilde{l} \sin \tilde{r}, \\ Y^1 &= \sinh \theta \cosh \tilde{l} \cos \tilde{r} - \cosh \theta \sinh \tilde{l} \sin \tilde{r}, & Y^2 &= \sinh \theta \cosh \tilde{l} \sin \tilde{r} + \cosh \theta \sinh \tilde{l} \cos \tilde{r} \end{aligned} \quad (2.98)$$

satisfy the quadric

$$Y^{0'}Y^1 - Y^0Y^2 = \sinh \theta \cosh \theta . \quad (2.99)$$

This surface is shown in the plot 3(g). It describes an infinite open string with two ends on the conformal boundary.

Case 3.4 $\langle LL \rangle = 0, \langle RR \rangle > 0$.

This case corresponds to the open line segment between the points B and C in fig. 2(b). Here $\rho^2 = \sin^2 \phi$ and $\phi \in (\pi/4, \pi/2)$. One obviously gets the same picture as in 3.2, since these two cases are related to each other by exchange of the left and right elements.

Case 3.5 $\langle LL \rangle = 0, \langle RR \rangle = 0$.

This corresponds to the point C in fig. 2(b), with $\rho^2 = 1/2$ and $\phi = \pi/4$. From (2.53) then follows: $l = \frac{1}{\sqrt{2}}(\tau + \sigma)$ and $r = \frac{1}{\sqrt{2}}(\tau - \sigma)$.

The pair (2.83) here reduces to

$$L = \frac{1}{2}(\mathbf{t}_2 + \mathbf{t}_0) , \quad R = \frac{1}{2}(\mathbf{t}_2 - \mathbf{t}_0) , \quad (2.100)$$

and by (2.50) we obtain the solution

$$g = e^{\frac{\sqrt{2}}{4}(\tau+\sigma)(\mathbf{t}_2+\mathbf{t}_0)} e^{\frac{\sqrt{2}}{4}(\tau-\sigma)(\mathbf{t}_2-\mathbf{t}_0)} = \frac{1}{4} \begin{pmatrix} 4 - \sigma^2 + \tau^2 + 2\sqrt{2}\tau & \sigma^2 - \tau^2 + 2\sqrt{2}\sigma \\ \sigma^2 - \tau^2 - 2\sqrt{2}\sigma & 4 - \sigma^2 + \tau^2 - 2\sqrt{2}\tau \end{pmatrix} . \quad (2.101)$$

The quadric (2.60) now yields

$$(Y^{0'} + Y^1)^2 = 1 , \quad (2.102)$$

and the embedding coordinates

$$Y^{0'} = 1 - \frac{\sigma^2 - \tau^2}{4} , \quad Y^0 = \frac{\sqrt{2}}{2}\sigma , \quad Y^1 = \frac{\sigma^2 - \tau^2}{4} , \quad Y^2 = \frac{\sqrt{2}}{2}\tau \quad (2.103)$$

realize (2.102) in the linear form $Y^{0'} + Y^1 = 1$. This surface is given by the plot 3(f).

Case 3.6 $\langle LL \rangle = 0, \langle RR \rangle < 0$.

This corresponds to the open segment between the points C and D in fig. 2(b).

Here $\rho^2 = \sin^2 \phi < \cos^2 \phi$, i.e. $\cos \phi = \sqrt{1 - \rho^2}$, $\phi \in (0, \pi/4)$ and $\rho^2 < 1/2$.

We follow the scheme of the case 3.2. The pair (2.83) now becomes

$$L = \rho\sqrt{1 - \rho^2}(\mathbf{t}_2 + \mathbf{t}_0) , \quad R = \rho^2\mathbf{t}_2 - (1 - \rho^2)\mathbf{t}_0 , \quad (2.104)$$

and one has the representation $R = -\sqrt{1 - 2\rho^2}e^{-\gamma\mathbf{t}_1}\mathbf{t}_0e^{\gamma\mathbf{t}_1}$, with $e^{-2\gamma} = (1 - 2\rho^2)^{-\frac{1}{2}}$. This leads to the solution

$$g = e^{\tilde{l}(\mathbf{t}_2+\mathbf{t}_0)} e^{-\tilde{r}\mathbf{t}_0} = \begin{pmatrix} (1 + \tilde{l}) \cos \tilde{r} + \tilde{l} \sin \tilde{r} & \tilde{l} \cos \tilde{r} - (1 + \tilde{l}) \sin \tilde{r} \\ (1 - \tilde{l}) \sin \tilde{r} - \tilde{l} \cos \tilde{r} & \tilde{l} \sin \tilde{r} + (1 - \tilde{l}) \cos \tilde{r} \end{pmatrix} , \quad (2.105)$$

where \tilde{l} and \tilde{r} are the rescaled coordinates

$$\tilde{l} = \frac{\rho \sqrt{1 - \rho^2}}{\sqrt{1 - 2\rho^2}} l, \quad \tilde{r} = \sqrt{1 - 2\rho^2} r. \quad (2.106)$$

The embedding coordinates for (2.105) are

$$Y^{0'} = \tilde{l} \sin \tilde{r} + \cos \tilde{r}, \quad Y^0 = \tilde{l} \cos \tilde{r} - \sin \tilde{r}, \quad Y^1 = -\tilde{l} \sin \tilde{r}, \quad Y^2 = \tilde{l} \cos \tilde{r}, \quad (2.107)$$

and they satisfy the quadric

$$(Y^{0'} + Y^1)^2 + (Y^0 - Y^2)^2 = 1. \quad (2.108)$$

This surface is given by the plot 3(h). It also describes an infinite open string, but in contrast to the case 3.3, now the end points coincide at the boundary.

Case 3.7 $\langle LL \rangle < 0$, $\langle RR \rangle > 0$.

This corresponds to the area inside the triangle BCE in fig. 2(b).

Here $\sin^2 \phi \cos^2 \phi < \rho^2(1 - \rho^2)$, $\phi \in (\pi/4, \pi/2)$, and one has the same picture as in 3.3.

Case 3.8 $\langle LL \rangle < 0$, $\langle RR \rangle = 0$.

This corresponds to the open segment between the points C and E in fig. 2(b).

Here $\sin^2 \phi > \rho^2 = \cos^2 \phi$, $\phi \in (\pi/4, \pi/2)$, and the picture is the same as in 3.6.

Case 3.9 $\langle LL \rangle < 0$, $\langle RR \rangle < 0$.

This corresponds to the area inside the triangle DCE in fig. 2(b).

Here $\rho^2 < \min[\sin \phi, \cos \phi]$ and it implies $\rho^2(1 - \rho^2) < \sin^2 \phi \cos^2 \phi$.

Writing the pair (2.83) as in (2.95)

$$L = \sqrt{\sin^2 \phi - \rho^2} e^{-\beta \mathbf{t}_1} \mathbf{t}_0 e^{\beta \mathbf{t}_1}, \quad R = -\sqrt{\cos^2 \phi - \rho^2} e^{-\gamma \mathbf{t}_1} \mathbf{t}_0 e^{\gamma \mathbf{t}_1}, \quad (2.109)$$

one obtains the solution

$$g = e^{\tilde{l} \mathbf{t}_0} e^{\theta \mathbf{t}_1} e^{-\tilde{r} \mathbf{t}_0} = \begin{pmatrix} \sinh \theta \sin \xi + \cosh \theta \cos \eta & \cosh \theta \sin \eta + \sinh \theta \cos \xi \\ \sinh \theta \cos \xi - \cosh \theta \sin \eta & \cosh \theta \cos \eta - \sinh \theta \sin \xi \end{pmatrix}, \quad (2.110)$$

where $\tilde{l} = \sqrt{\sin^2 \phi - \rho^2} l$, and $\tilde{r} = \sqrt{\cos^2 \phi - \rho^2} r$ are the rescaled coordinates, $\xi = \tilde{l} + \tilde{r}$, $\eta = \tilde{l} - \tilde{r}$, and $\theta = \beta - \gamma$ is defined by

$$\tanh 2\theta = \frac{\rho \sqrt{1 - \rho^2}}{\sin \phi \cos \phi}. \quad (2.111)$$

The embedding coordinates

$$Y^{0'} = \cosh \theta \cos \eta, \quad Y^0 = \cosh \theta \sin \eta, \quad Y^1 = \sinh \theta \cos \xi, \quad Y^2 = \sinh \theta \sin \xi \quad (2.112)$$

satisfy the quadric

$$(Y^1)^2 + (Y^2)^2 = \sinh^2 \theta . \quad (2.113)$$

This surface is shown in the plot 3(i). Only this case does not extend to the boundary of AdS_3 .

At the end of this section we comment on the solution (2.50) in the general time-like case with the pair (L, R) given by (2.83). The simple rules for the exponentiation of the $\mathfrak{sl}(2, \mathbb{R})$ elements (see appendix A) enable us to calculate the exponents in (2.50) and then find the embedding coordinates. In the domain bounded by the triangle ABC in fig. 2(a), this calculation leads to the answer

$$\begin{aligned} Y^{0'} &= \cosh(\lambda l) \cosh(\mu r) - \sin \phi \cos \phi \frac{\sinh(\lambda l)}{\lambda} \frac{\sinh(\mu r)}{\mu} , \\ Y^0 &= \sqrt{1 - \rho^2} \sin \phi \frac{\sinh(\lambda l)}{\lambda} \cosh(\mu r) + \sqrt{1 - \rho^2} \cos \phi \cosh(\lambda l) \frac{\sinh(\mu r)}{\mu} , \\ Y^1 &= \rho \sqrt{1 - \rho^2} \frac{\sinh(\lambda l)}{\lambda} \frac{\sinh(\mu r)}{\mu} , \\ Y^2 &= \rho \cos \phi \frac{\sinh(\lambda l)}{\lambda} \cosh(\mu r) - \rho \sin \phi \cosh(\lambda l) \frac{\sinh(\mu r)}{\mu} , \end{aligned} \quad (2.114)$$

where $\lambda = \sqrt{\rho^2 - \sin^2 \phi}$ and $\mu = \sqrt{\rho^2 - \cos^2 \phi}$.

Note that λ and μ vanish at the edges BC and AC , respectively. However, the solution (2.114) remains regular there, and has a smooth continuation to other domains of the square $\rho^2 < 1$. When crossing the diagonals of the square one has to replace the hyperbolic functions with the corresponding trigonometric ones. This means that in any compact domain of AdS_3 the different solutions are smoothly related to each other via variations of the parameters ρ and ϕ . However, the solutions differ essentially in their global properties which are reflected at the boundary of AdS_3 . We analyze the boundary behavior of the solutions in section 4.

In the next section we consider the scheme of Pohlmeyer reduction for the time-like and light-like surfaces and establish a connection with the group theoretical treatment of this section. Namely we show how the general cases described by eqs. (2.81) and (2.114) are reproduced by the Pohlmeyer reduction.

3 Analysis via Pohlmeyer reduction

In this section we treat minimal space-like surfaces in $\text{AdS}_3 \times \text{S}^3$ within the framework of the Pohlmeyer reduction. As it was mentioned above, the AdS_3 projection of a space-like surface in $\text{AdS}_3 \times \text{S}^3$ may be space-like, time-like, or even light-like. The S^3 part and the case of space-like AdS_3 was studied in [6]. Here we consider the time-like and light-like cases.

3.1 Time-like AdS_3 projection

We realize the AdS_3 space as the hyperboloid (2.2) embedded in $\mathbb{R}^{2,2}$. Using conformal worldsheet coordinates on $\text{AdS}_3 \times \text{S}^3$ one gets the following equation for the AdS_3 projection

$$\bar{\partial} \partial Y = (\partial Y \cdot \bar{\partial} Y) Y . \quad (3.1)$$

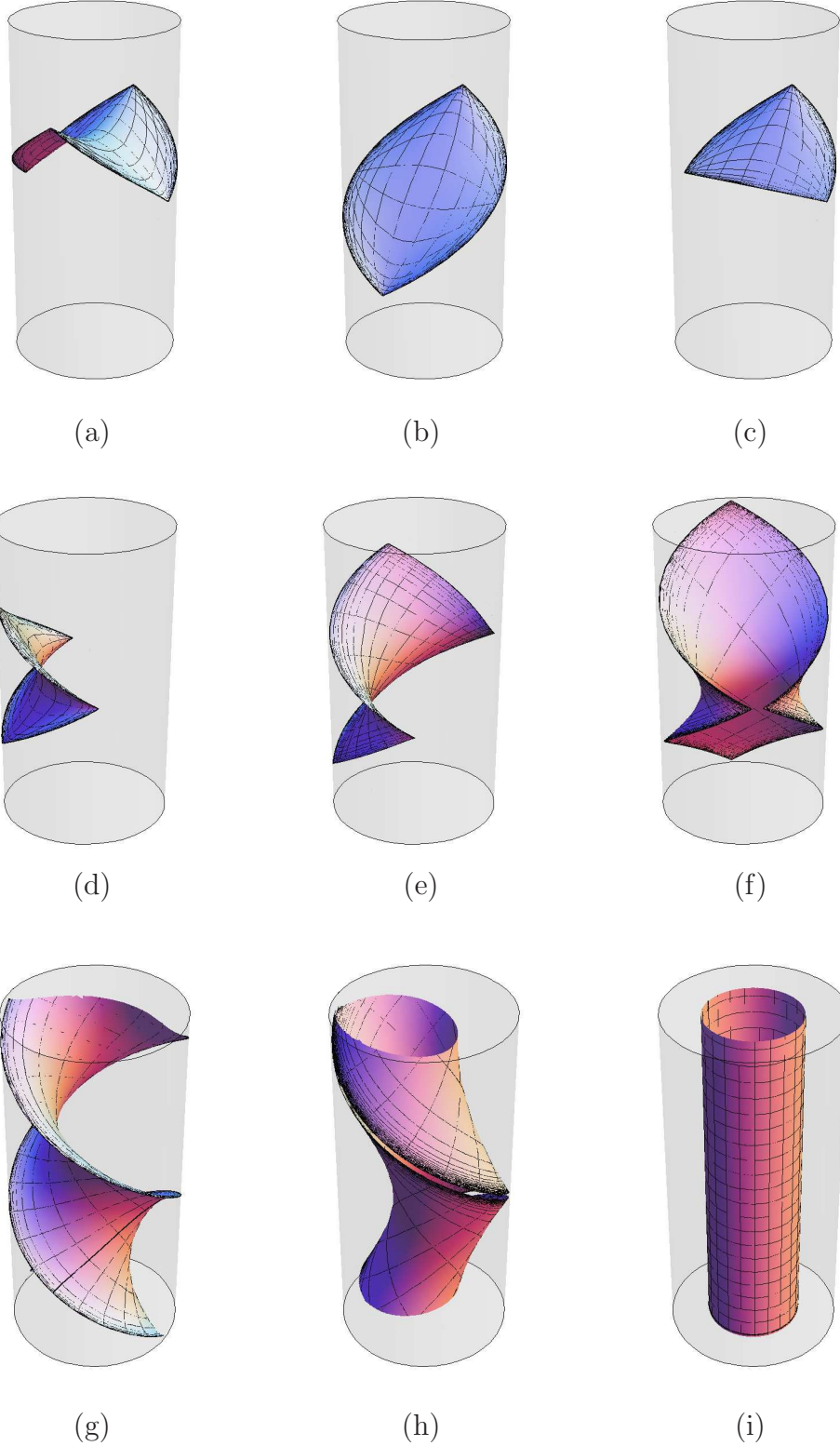


Figure 3: Different vacuum string surfaces in AdS_3 described in section 2.4. The correspondence to formulas is: (a) - (2.66), (b) - (2.72), (c) - (2.79), (d) - (2.88), (e) - (2.93), (f) - (2.103), (g) - (2.98), (h) - (2.107), (i) - (2.112).

The gauge fixing conditions (2.12) can be written as

$$\partial Y \cdot \partial Y = -1 = \bar{\partial} Y \cdot \bar{\partial} Y , \quad (3.2)$$

and in the real worldsheet coordinates (σ, τ) this means

$$(\partial_\tau Y)^2 - (\partial_\sigma Y)^2 = 1 , \quad \partial_\sigma Y \cdot \partial_\tau Y = 0 . \quad (3.3)$$

We assume that $\partial_\sigma Y$ is time-like $\partial_\sigma Y \cdot \partial_\sigma Y < 0$ and $\partial_\tau Y$ is space-like $\partial_\tau Y \cdot \partial_\tau Y > 0$. These conditions yield $-1 < \partial Y \cdot \bar{\partial} Y < 1$ and one can use the parameterization

$$\partial Y \cdot \bar{\partial} Y = \cos \alpha . \quad (3.4)$$

We introduce the basis $\mathcal{B} = \{Y, \partial Y, \bar{\partial} Y, N\}$ in $\mathbb{R}^{2,2}$, where N is the normalized orthogonal vector to the surface

$$N \cdot N = 1 , \quad Y \cdot N = \partial Y \cdot N = \bar{\partial} Y \cdot N = 0 . \quad (3.5)$$

The real vector N has to be space-like, since the worldsheet in AdS_3 is time-like.

Differentiating with respect to z on gets the linear equations

$$\begin{aligned} \partial^2 Y &= -Y + \frac{\partial \alpha}{\sin \alpha} (\cos \alpha \partial Y + \bar{\partial} Y) + u N , \\ \partial \bar{\partial} Y &= \cos \alpha Y , \\ \partial N &= \frac{u}{\sin^2 \alpha} (\partial Y + \cos \alpha \bar{\partial} Y) , \end{aligned} \quad (3.6)$$

where

$$u = \partial^2 Y \cdot N \quad (3.7)$$

is the zz -component of the second fundamental form. Introducing also the equations complex conjugated to (3.6), one finds the consistency conditions for the linear system

$$\begin{aligned} \partial \bar{\partial} \alpha &= \sin \alpha - \frac{u \bar{u}}{\sin \alpha} , \\ \bar{\partial} u &= -\frac{\partial \alpha}{\sin \alpha} \bar{u} , \quad \partial \bar{u} = -\frac{\bar{\partial} \alpha}{\sin \alpha} u . \end{aligned} \quad (3.8)$$

In the next subsection we describe constant solutions of these equations and integrate the corresponding linear system (3.6).

3.2 Integration of the linear system

Due to the consistency conditions (3.8) constant α implies constant u and we parameterize

$$u = u_0 , \quad \sin^2 \alpha = |u_0|^2 , \quad (3.9)$$

$$u_0 = \frac{2}{i} \rho \sqrt{1 - \rho^2} e^{2i\phi} , \quad 0 < \rho < 1 . \quad (3.10)$$

The induced metric tensor $f_{ab} = \partial_a Y \cdot \partial_b Y$ and the second fundamental form $U_{ab} = \partial_{ab}^2 Y \cdot N$ corresponding to the solution (3.9)-(3.10) become

$$f_{ab}(\sigma, \tau) = \begin{pmatrix} \rho^2 - 1 & 0 \\ 0 & \rho^2 \end{pmatrix}, \quad U_{ab} = \rho \sqrt{1 - \rho^2} \begin{pmatrix} \sin 2\phi & \cos 2\phi \\ \cos 2\phi & -\sin 2\phi \end{pmatrix}. \quad (3.11)$$

This form of the metric tensor (compare with (2.49)) justifies the parameterization of the norm of u_0 by ρ . One can show that the angle variable in (3.10) also coincides with ϕ used in the previous section. This implies for the mean curvature of the AdS₃ projection (θ defined as in (2.87))⁶

$$H = \frac{1}{2}(f^{-1})_{ab}U_{ab} = -\frac{\sin 2\phi}{2\rho\sqrt{1-\rho^2}} = -\coth 2\theta. \quad (3.12)$$

Let us introduce the following real orthonormal basis vectors

$$\mathcal{E}_{0'} = Y, \quad \mathcal{E}_0 = \frac{\partial_1 Y}{\sqrt{1-\rho^2}}, \quad \mathcal{E}_1 = N, \quad \mathcal{E}_2 = \frac{\partial_2 Y}{\rho}. \quad (3.13)$$

They satisfy the conditions $\mathcal{E}_J \cdot \mathcal{E}_K = G_{JK}$, where G_{JK} is the metric tensor of $\mathbb{R}^{2,2}$. Hence, the matrix $\mathcal{E}_J{}^K$ built from vector components is in $O(2, 2)$. The system (3.6) is then equivalent to the matrix equations

$$\partial_a \mathcal{E}_J{}^K = (\mathcal{A}_a)_J{}^{J'} \mathcal{E}_{J'}{}^K \quad (a = 1, 2). \quad (3.14)$$

The matrices \mathcal{A}_a belong to the $\mathfrak{so}(2, 2)$ algebra and they have the following block structure

$$\mathcal{A}_1 = \begin{pmatrix} C_1 & B_1 \\ B_1^T & D_1 \end{pmatrix}, \quad \mathcal{A}_2 = \begin{pmatrix} 0 & B_2 \\ B_2^T & D_2 \end{pmatrix}, \quad (3.15)$$

with 2×2 matrices

$$B_1 = \begin{pmatrix} 0 & 0 \\ \rho \sin 2\phi & 0 \end{pmatrix}, \quad B_2 = \begin{pmatrix} 0 & \rho \\ \rho \cos 2\phi & 0 \end{pmatrix}, \quad (3.16)$$

$$C_1 = \sqrt{1 - \rho^2} \mathbf{t}_0, \quad D_1 = -\sqrt{1 - \rho^2} \cos 2\phi \mathbf{t}_0, \quad D_2 = \sqrt{1 - \rho^2} \sin 2\phi \mathbf{t}_0. \quad (3.17)$$

The integrability of the system (3.14) is provided by $[\mathcal{A}_1, \mathcal{A}_2] = 0$, and one obtains

$$\mathcal{E} = \exp(\xi^a \mathcal{A}_a) C, \quad (3.18)$$

where C is a constant $O(2, 2)$ matrix.

To perform the exponentiation we use the decomposition $\mathfrak{so}(2, 2) = \mathfrak{sl}(2, \mathbb{R}) \oplus \mathfrak{sl}(2, \mathbb{R})$, described in appendix B. The basis of this decomposition can be chosen as

$$\begin{aligned} (L_0)_J{}^K &= \begin{pmatrix} \mathbf{t}_0 & 0 \\ 0 & \mathbf{t}_0 \end{pmatrix}, & (L_1)_J{}^K &= \begin{pmatrix} 0 & \mathbf{t}_2 \\ \mathbf{t}_2 & 0 \end{pmatrix}, & (L_2)_J{}^K &= \begin{pmatrix} 0 & \mathbf{t}_1 \\ \mathbf{t}_1 & 0 \end{pmatrix}, \\ (R_0)_J{}^K &= \begin{pmatrix} -\mathbf{t}_0 & 0 \\ 0 & \mathbf{t}_0 \end{pmatrix}, & (R_1)_J{}^K &= \begin{pmatrix} 0 & -\mathbf{I} \\ -\mathbf{I} & 0 \end{pmatrix}, & (R_2)_J{}^K &= \begin{pmatrix} 0 & -\mathbf{t}_0 \\ \mathbf{t}_0 & 0 \end{pmatrix}. \end{aligned} \quad (3.19)$$

⁶Taking the conformal metric of the surface instead of f_{ab} will of course provide a vanishing mean curvature due to minimality of the surface as a whole.

The matrices L_μ ($\mu = 0, 1, 2$) and R_ν ($\nu = 0, 1, 2$) commute: $[L_\mu, R_\nu] = 0$, and in addition they satisfy the algebraic relations similar to (2.5)

$$L_\mu L_\nu = \eta_{\mu\nu} I - \epsilon_{\mu\nu}{}^\rho L_\rho, \quad R_\mu R_\nu = \eta_{\mu\nu} I - \epsilon_{\mu\nu}{}^\rho R_\rho. \quad (3.20)$$

The expansion of the matrices \mathcal{A}_a in the basis (3.19) takes the form

$$\mathcal{A}_1 = \sin \phi (\rho \cos \phi L_2 + \sqrt{1 - \rho^2} \sin \phi L_0) + \cos \phi (\rho \sin \phi R_2 - \sqrt{1 - \rho^2} \cos \phi R_0), \quad (3.21)$$

$$\mathcal{A}_2 = \cos \phi (\rho \cos \phi L_2 + \sqrt{1 - \rho^2} \sin \phi L_0) - \sin \phi (\rho \sin \phi R_2 - \sqrt{1 - \rho^2} \cos \phi R_0),$$

and the exponential in (3.18) becomes

$$\exp[l(\rho \cos \phi L_2 + \sqrt{1 - \rho^2} \sin \phi L_0) + r(\rho \sin \phi R_2 - \sqrt{1 - \rho^2} \cos \phi R_0)], \quad (3.22)$$

where l and r are given by (2.53). The calculation of (3.22) can be done similarly to the $\mathfrak{sl}(2, \mathbb{R})$ case. The solution $Y(\sigma, \tau)$ is defined by the first row of (3.18). Taking $C = I$, one obtains just (2.114). In appendix B we give an alternative proof of the same statement, which establishes direct relation between the two integration methods.

3.3 Light-like AdS₃ projection

The induced metric on a light-like AdS₃ projection

$$f_{ab} = \begin{pmatrix} 0 & 0 \\ 0 & 1 \end{pmatrix} \quad (3.23)$$

is obtained from (3.11) in the limit $\rho \rightarrow 1$, and it corresponds to a light-like tangent vector $\partial_\sigma Y$. Due to this light-like tangent vector the usual definition of the normal direction via orthogonality conditions or constructions with ϵ -tensor break down. Instead one can fix unambiguously a normal vector in a covariant way by the conditions

$$N \cdot Y = N \cdot \partial_\tau Y = N \cdot N = 0, \quad N \cdot \partial_\sigma Y = \frac{1}{2}. \quad (3.24)$$

Then we introduce the orthonormal basis

$$\mathcal{E}_0' = Y, \quad \mathcal{E}_0 = \partial_\sigma Y - N, \quad \mathcal{E}_1 = \partial_\sigma Y + N, \quad \mathcal{E}_2 = \partial_\tau Y. \quad (3.25)$$

The linear system for this basis takes the standard form (3.14)

$$\partial_\sigma \mathcal{E} = \mathcal{A}_\sigma \mathcal{E}, \quad \partial_\tau \mathcal{E} = \mathcal{A}_\tau \mathcal{E}, \quad (3.26)$$

with the $\mathfrak{so}(2, 2)$ matrices

$$\mathcal{A}_\sigma = \begin{pmatrix} 0 & 1/2 & 1/2 & 0 \\ -1/2 & 0 & 2u_{\sigma\sigma} & u_{\tau\sigma} \\ 1/2 & 2u_{\sigma\sigma} & 0 & -u_{\tau\sigma} \\ 0 & u_{\tau\sigma} & u_{\tau\sigma} & 0 \end{pmatrix}, \quad \mathcal{A}_\tau = \begin{pmatrix} 0 & 0 & 0 & 1 \\ 0 & 0 & 2u_{\tau\sigma} & -u_{\sigma\sigma} \\ 0 & 2u_{\tau\sigma} & 0 & u_{\sigma\sigma} \\ 1 & -u_{\sigma\sigma} & -u_{\sigma\sigma} & 0 \end{pmatrix}, \quad (3.27)$$

where $u_{\sigma\sigma} = N \cdot \partial_\sigma \partial_\sigma Y = -N \cdot \partial_\tau \partial_\tau Y$ and $u_{\tau\sigma} = N \cdot \partial_\tau \partial_\sigma Y$ are the coefficients of the second fundamental form. Note that this analysis implies that all second derivatives of Y are linear combinations only of Y and $\partial_\sigma Y$ and hence as vectors from the AdS point of view parallel to $\partial_\sigma Y$. This in agreement with the analogous situation in the group theoretical treatment above. The consistency conditions for (3.26) yield the equations

$$\partial_\tau u_{\sigma\sigma} = \partial_\sigma u_{\tau\sigma} , \quad \partial_\sigma u_{\sigma\sigma} + \partial_\tau u_{\tau\sigma} + 2u_{\sigma\sigma}^2 + 2u_{\tau\sigma}^2 - \frac{1}{2} = 0 , \quad (3.28)$$

which are equivalent to (2.56) with $u_{\sigma\sigma} = a$, $u_{\tau\sigma} = b - 1/2$, and they allow non constant solutions as well.

The vacuum surfaces are associated with constant $u_{\sigma\sigma}$ and $u_{\tau\sigma}$. In this case (3.28) reduces to $u_{\sigma\sigma}^2 + u_{\tau\sigma}^2 = 1/4$ and one can use the parameterization $u_{\sigma\sigma} = \frac{1}{2} \sin 2\phi$ and $u_{\tau\sigma} = \frac{1}{2} \cos 2\phi$.

Since the metric induced from AdS₃ is degenerate, the mean curvature as a standard invariant geometric quantity is ill defined. To relate the information carried by ϕ to an invariant, one could replace $(f^{-1})_{ab}$ in the definition of the mean curvature by $(f_s^{-1})_{ab}$. In any case, ϕ has meaning only for the mutual relation of AdS₃ and S³ projection. The expansion of the matrices (3.27) in the basis (3.19) now becomes

$$\begin{aligned} \mathcal{A}_\sigma &= \sin \phi (\cos \phi L_2 + \sin \phi L_+) + \cos \phi (\sin \phi R_2 - \cos \phi R_+) , \\ \mathcal{A}_\tau &= \cos \phi (\cos \phi L_2 + \sin \phi L_+) - \sin \phi (\sin \phi R_2 - \cos \phi R_+) , \end{aligned} \quad (3.29)$$

where $L_+ = \frac{1}{2}(L_0 + L_1)$ and $R_+ = \frac{1}{2}(R_0 + R_1)$. The left-right decomposition simplifies the calculation of the exponent $\exp(\sigma \mathcal{A}_\sigma + \tau \mathcal{A}_\tau)$, and one finds that its first row is given by (2.81), like for the time-like surfaces. The cases $\phi = 0$ and $\phi = \pi/2$ have to be treated separately and they reproduce (2.72) and (2.75), respectively.

The derivation of the equivalence between the Pohlmeyer reduction and group variable construction, presented in appendix B, is valid for this case as well.

Now we describe light-like AdS₃ string surfaces in the general case (with non-constant $u_{\sigma\sigma}$ and $u_{\tau\sigma}$). For this purpose let us consider the analog of the linear system (3.6), which now takes the form

$$\begin{aligned} \partial^2 Y &= -Y + u(\partial Y + \bar{\partial} Y) , \\ \partial \bar{\partial} Y &= Y , \\ \partial N &= \frac{Y}{2} + \frac{u}{4} (\partial Y - \bar{\partial} Y) - uN , \end{aligned} \quad (3.30)$$

where $u = \partial^2 Y \cdot N$ and N is defined by (3.24). We will use only the first two equations. From them follows that $\partial(\partial Y + \bar{\partial} Y) = u(\partial Y + \bar{\partial} Y)$, and, therefore, the light-like vector $\partial_\sigma Y = \frac{1}{2}(\partial Y + \bar{\partial} Y)$ can be written as $\partial_\sigma Y = \psi e_+$, with a constant e_+ and an arbitrary scalar function ψ . For $e_+ = (0, 1, 1, 0)$, which one can choose using the O(2, 2) transformations, the vector Y becomes $Y = (\cosh \gamma, F, F, \sinh \gamma)$, where γ depends only on τ and $\partial_\sigma F = \psi$. Then, from the second equation of (3.30) follows $\gamma = \tau$ and F satisfies the free field equation

$$\bar{\partial} \partial F = F . \quad (3.31)$$

Thus, the general light-like AdS₃ surface, up to O(2, 2) transformations, is given by

$$Y^0 = \cosh \tau , \quad Y^0 = F(\sigma, \tau) , \quad Y^1 = F(\sigma, \tau) , \quad Y^2 = \sinh \tau . \quad (3.32)$$

Being interested in the AdS projection only, this surface satisfies the same quadric as the constant u light-like surfaces.

Concluding this section note that the consistency conditions for the system (3.30) reads

$$\bar{\partial}u + u\bar{u} = 1, \quad \partial\bar{u} + u\bar{u} = 1, \quad (3.33)$$

which is equivalent to (3.28) with $u = 2(u_{\sigma\sigma} - iu_{\tau\sigma})$. According to the construction above, these consistency conditions are solved by $u = \partial\psi/\psi$.

3.4 Relation to complex $\sin(\mathfrak{h})$ -Gordon models

We will now discuss the Lagrangean structure of the consistency conditions. It is well known that Pohlmeyer reduction of sigma models on S^3 and AdS_3 leads to complex sine-Gordon and complex sinh-Gordon models, respectively [8]. Considering space-like strings on $\text{AdS}_3 \times S^3$ with different signatures of the induced metric tensor on the AdS projection, one obtains various modifications of these models on Euclidean worldsheets. All these models are Lagrangean. Below we present the Lagrange functions and the corresponding simple solutions related to our string configurations.

Let us consider the case of a time-like AdS projection. The consistency conditions (3.8) allow a parameterization of u and \bar{u} by one real field φ (and the field α) in the following form

$$u = \partial\varphi \tan(\alpha/2), \quad \bar{u} = \bar{\partial}\varphi \tan(\alpha/2). \quad (3.34)$$

The obtained two second order differential equations for α and φ are Lagrangean with

$$\mathcal{L} = \frac{1}{2} \partial\alpha \bar{\partial}\alpha - \frac{1}{2} \tan^2(\alpha/2) \partial\varphi \bar{\partial}\varphi - \cos\alpha. \quad (3.35)$$

In terms of the new fields

$$\psi_{\pm} = e^{\pm\frac{\varphi}{2}} \sin(\alpha/2), \quad (3.36)$$

the Lagrangian (3.35) becomes algebraic

$$\mathcal{L} = \frac{\partial\psi_+ \bar{\partial}\psi_- + \bar{\partial}\psi_+ \partial\psi_-}{1 - \psi_+ \psi_-} - 2\psi_+ \psi_-, \quad (3.37)$$

and the constant solution (3.10) corresponds to

$$\psi_{\pm} = \sqrt{1 - \rho^2} e^{\pm\rho^2 [\cos(2\phi)\tau + \sin(2\phi)\sigma]}. \quad (3.38)$$

In the case of light-like AdS_3 projection (see (3.33)) one can introduce the parameterization $u = \partial\psi/\psi$, $\bar{u} = \bar{\partial}\psi/\psi$, with real ψ , which satisfies the linear equation $\bar{\partial}\partial\psi = \psi$. Thus, the Lagrangian here is quadratic

$$\mathcal{L} = \partial\psi \bar{\partial}\psi + \psi^2, \quad (3.39)$$

and our constant solution $u = -ie^{2i\phi}$ corresponds to $\psi = e^{\cos(2\phi)\tau + \sin(2\phi)\sigma}$.

One can similarly derive a Lagrangian system for the space-like AdS projection. Instead of (3.35) one now gets the complex sinh-Gordon model with

$$\mathcal{L} = \frac{\partial\psi_+ \bar{\partial}\psi_- + \bar{\partial}\psi_+ \partial\psi_-}{1 + \psi_+ \psi_-} + 2\psi_+ \psi_- . \quad (3.40)$$

Here ψ_{\pm} parameterize the first and the second fundamental forms as in (3.34) and (3.36), replacing there the trigonometric functions by hyperbolic ones. The solution for ψ_{\pm} is also obtained from (3.38) by changing the sign under the square root, that keeps (3.38) real.

Finally, for the spherical part one has the consistency conditions (see for example in [6])

$$\partial\bar{\partial}\beta + \sinh\beta - \frac{v\bar{v}}{\sinh\beta} = 0 , \quad \bar{\partial}v - \frac{\partial\beta}{\sinh\beta}\bar{v} = 0 , \quad (3.41)$$

where $v = M \cdot \partial^2 X$ (with normal vector M) is the coefficient of the second fundamental form and β parameterizes the induced metric on the S^3 projection like α on AdS_3

$$(f_s)_{ab} = \begin{pmatrix} \cosh^2(\beta/2) & 0 \\ 0 & \sinh^2(\beta/2) \end{pmatrix} . \quad (3.42)$$

Then, in a similar way (with $v = i\partial\varphi_s \tanh(\beta/2)$) one finds the Lagrangian

$$\mathcal{L} = \frac{\partial\psi \bar{\partial}\bar{\psi} + \bar{\partial}\psi \partial\bar{\psi}}{1 + \psi \bar{\psi}} - 2\psi \bar{\psi} , \quad (3.43)$$

with a complex field

$$\psi = e^{\frac{i\varphi_s}{2}} \sinh(\beta/2) . \quad (3.44)$$

Constant solutions of (3.41) leading to (2.43) correspond to $\psi = \rho_s e^{i\sqrt{1+\rho_s^2} [\sin(2\phi_s)\tau - \cos(2\phi_s)\sigma]}$.

4 Analysis of the boundaries

For the investigation of the boundary behavior of our surfaces it is very convenient to use their description as (part of the) intersections of quadrics with the AdS_3 hyperboloid in $\mathbb{R}^{(2,2)}$. Global AdS_3 coordinates just implementing the conformal map to one half of the Einstein static universe (ESU) are

$$Y^{0'} = \frac{1}{\cos\vartheta} \sin t , \quad Y^0 = \frac{1}{\cos\vartheta} \cos t , \quad Y^1 = \tan\vartheta \cos\gamma , \quad Y^2 = \tan\vartheta \sin\gamma , \quad (4.1)$$

with $0 \leq \vartheta < \frac{\pi}{2}$, $0 \leq \gamma < 2\pi$, $-\pi \leq t < \pi$. This map is the basis for the fig. 3, $\vartheta = \frac{\pi}{2}$ corresponds to the boundary of AdS_3 . We demonstrate the procedure with a combined discussion of the space-like and time-like tetragon solution, fig. 3(a) and 3(d).

Here the quadrics (2.68) and (2.89) imply

$$\cos t = \pm \sqrt{\sin^2\vartheta \cos^2\gamma + \kappa \cos^2\vartheta} , \quad (4.2)$$

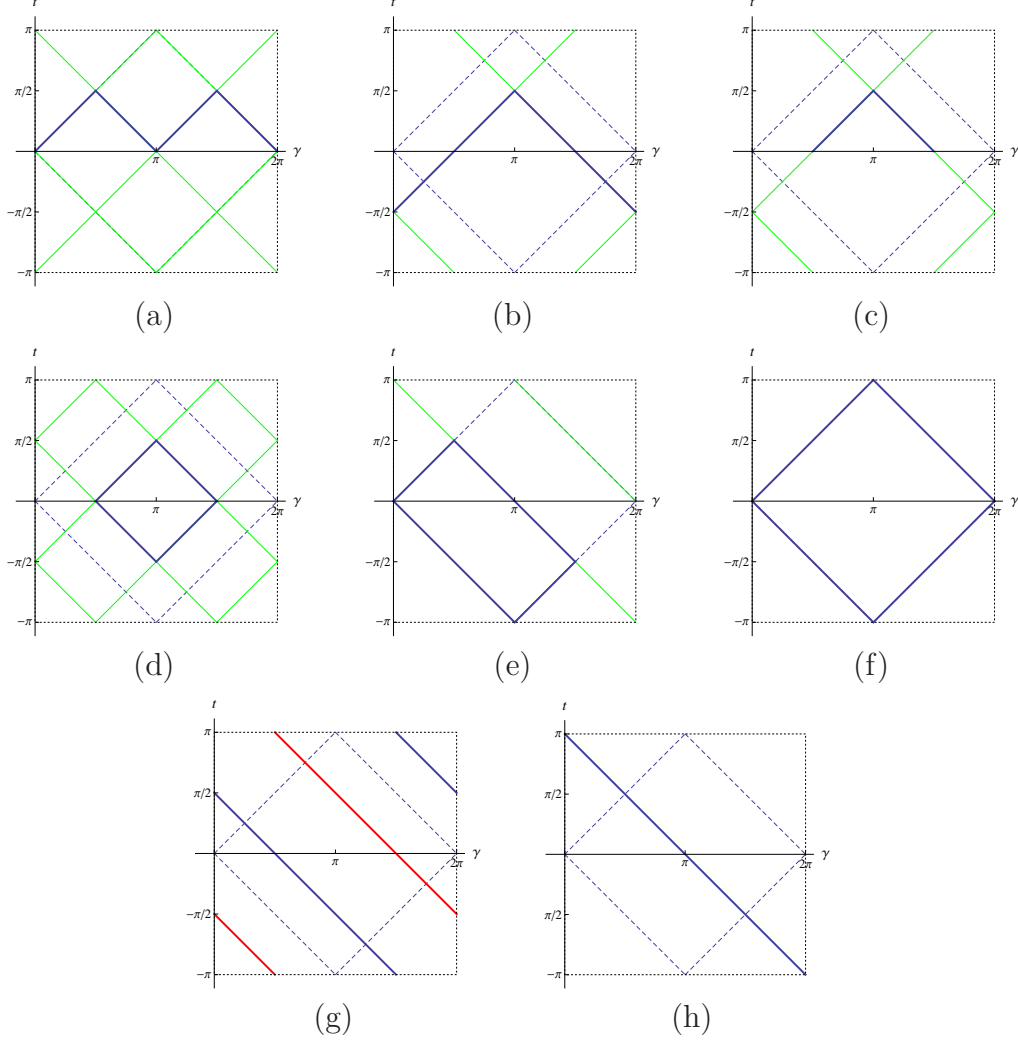


Figure 4: These are the conformal boundaries of all classes from fig. 3 that touch the boundary. Additionally, the dashed line is the boundary of a single Poincaré patch.

with $\kappa = \sin^2 \theta \in (0, \frac{1}{2}]$ in the space-like case and $\kappa = -\sinh^2 \theta < 0$ in the time-like case. Obviously, for the space-like case all values of ϑ inside the ESU cylinder are allowed, and for a given ϑ the angle variable γ can go around a full circle. On the other side, in the time-like case reality of the square root requires $|\kappa| \leq \tan^2 \vartheta$ and $\cos^2 \gamma \geq |\kappa| \cot^2 \vartheta$. Now there is an inner region of the ESU cylinder not reached by the surface, and beyond this region the allowed values for γ fall into two disjoint arcs of a circle.

In both cases, due to the symmetry and periodicity properties of $\cos t$, we see that to each allowed pair (ϑ, γ) belong just four different values in $t \in [-\pi, \pi)$, as long as $\vartheta < \frac{\pi}{2}$. Therefore, the intersections under discussion both consist out of four disconnected pieces touching each other only at the boundary. Each of these four pieces is a surface of the type depicted in fig. 3(a) or fig. 3(d), respectively.

Independent of the value of κ , (4.2) at the boundary of AdS_3 becomes $\cos t = \pm |\cos \gamma|$

which in $0 \leq \gamma < 2\pi$, $-\pi \leq t < \pi$ has the null line solutions

$$t = \pm\gamma, \quad t = \pi - \gamma, \quad t = -\pi + \gamma, \quad t = 2\pi - \gamma, \quad t = -2\pi + \gamma. \quad (4.3)$$

Out of this net of null lines the boundary of the four parts of the intersection of (2.68) (space-like case) with the hyperboloid is formed from four zigzag null lines going around the cylinder and each staying within a time slice of width $\frac{\pi}{2}$. For the intersection of (2.89) (time-like case) the boundaries are formed by four squares organized in two pairs with partners just being mirror images under reflection at the cylinder axis.

In fig. 4(a) and 4(d) we show the boundary configuration for one connected part of the intersections, i.e. for our previously constructed surfaces and depicted in fig. 3(a) and 3(d). An additional shift in time and γ has been implemented in the plot for graphical reasons in the time-like case. We also indicate in this and the following figures the boundary of a suitable chosen Poincaré patch, i.e. a conformal representation of two-dimensional Minkowski space. In a similar manner we can analyze the boundary behavior of all the other classes of surfaces shown in fig. 3. There are two light-like classes, fig. 3(b) and fig. 3(c), which we call the light-like two-gon and wedge, respectively. Their boundary is represented in fig. 4(b) and 4(c). The remaining time-like cases are also visualized in fig. 4. After this discussion let us summarize the properties of our classification. As indicated in fig. 2, to each point in the (ρ, ϕ) -diagram corresponds a projection of the surface onto AdS_3 plus all information allowing to reconstruct, together with the analogous input from the S^3 projection, the full solutions in $\text{AdS}_3 \times S^3$. This is true up to isometry transformations $\in O(2, 2)$. If one further is interested only in the AdS projection as a surface per se, points on the dashed lines in fig. 2 have to be identified. Then using the $O(2, 2)$ freedom we have generated for each class some simple explicit expressions for the embedding coordinates. Related to these representations are simple quadrics which define them as (parts of) intersections with the AdS_3 hyperboloid. In this manner we constructed within each class a canonical representative. While for parts of the classes the shape is fixed completely, for other classes there is a free parameter encoding the possible values for the constant mean curvature. The corresponding nine canonical AdS projections are shown in fig. 3. All other projections can be generated out of them by applying $O(2, 2)$ transformations (for illustration see fig. 5).

To summarize, in the following, we indicate the name, the corresponding position in fig. 3, the intersecting quadrics, the range for ρ and ϕ related to its positions in the diagram fig. 2 and its mean curvature. We also add the topological characterization of the boundary as (parts) of left and/or right going null lines on $\mathbb{R} \times S^1$.

Space-like tetragon, fig. 3(a):

$$Y_0^2 - Y_1^2 = \sin^2 \theta, \quad \text{region above line } AB, \quad H = \cot 2\theta, \\ \text{two left, two right.}$$

Light-like two-gon, fig. 3(b):

$$(Y^0 - Y^1)(Y^0 + Y^1) = 0, \quad \text{point } A \text{ or } B, \quad H \text{ ill defined,} \\ \text{one left, one right.}$$

Light-like wedge, fig. 3(c):

$Y_0^2 - Y_1^2 = 0$, open line segment AB , H ill defined,
one left, one right, part of boundary of the AdS projection inside.

Time-like tetragon, fig. 3(d):

$Y_0^2 - Y_1^2 = -\sinh^2 \theta$, interior of triangle ABC , $H = -\coth 2\theta$,
one left, one right.

Time-like special antisymmetric case, fig. 3(e):

$(Y^{0'} + Y^1)^2 - (Y^0 + Y^2)^2 = 1$, open line segments AC or BC , $H = -1$,
two left, one right *or* one left two right.

Time-like two-gon, fig. 3(f):

$(Y^{0'} + Y^1)^2 = 1$, point C , $H = -1$,
one left, one right.

Time-like two line case, fig. 3(g):

$Y^{0'}Y^1 - Y^0Y^2 = \frac{1}{2} \sinh 2\theta$, interior of triangles ACD or BCD , $H = -\tanh 2\theta$,
two left *or* two right.

Time-like one line case, fig. 3(h):

$(Y^{0'} + Y^1)^2 + (Y^0 - Y^2)^2 = 1$, open line segments CD or CE , $H = -1$,
one left *or* one right.

Time-like tube, fig. 3(i):

$Y_1^2 + Y_2^2 = \sinh^2 \theta$, interior of triangle DCE , $H = -\coth 2\theta$,
does not touch boundary of AdS.

Isometry transformations on AdS_3 can be continued to the conformal boundary where they act as conformal transformations. By conformal transformation one can change the distance of two parallel light-like lines. Using this we can deform the apparent shape with respect to the chosen coordinate system of the surfaces,⁷ but the geometric shape is of course untouched. For example, one can decrease the distance between the two lines in the two-line solution fig. 4(g) with a suitable isometry transformation. With an infinite boost, one can bring them exactly together and obtain the one-line solution fig. 4(h).

The boundary of the time-like tetragon fig. 4(d) solution consists of two left-moving and two right-moving lines. Using a boost one can decrease the distance between the right-moving lines and in the limit obtain the asymmetric solution fig. 4(f). There are further examples of how different classes of solutions are connected via infinite boosts.

⁷Just in the same sense in which one can in any finite domain of Minkowski space or AdS approximate a light ray by a ultrarelativistic massive particle trajectory.

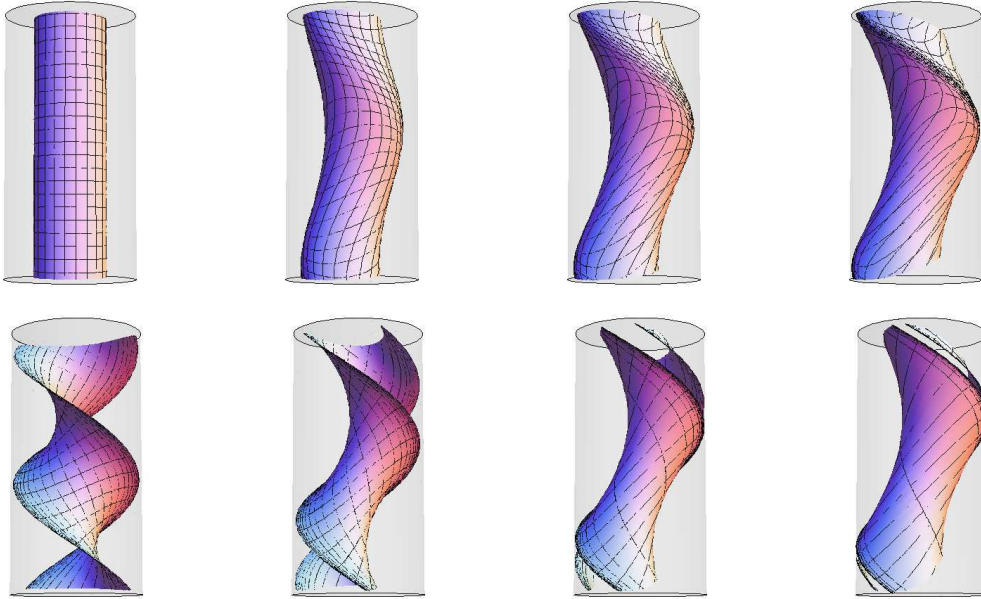


Figure 5: Via boosts one can change the apparent shape of the time-like tube and the time-like two line solution to look similar to a time-like one line surface.

5 Embedding in AdS_5 and a regularized area

For potential use in the correspondence to 4-point gluon scattering amplitudes, with generic kinematics in the center of mass system, one has to consider boundary null tetragons in 3-dimensional Minkowski space conformal to parts of the boundary of $\text{AdS}_4 \subset \text{AdS}_5$. Here beyond the space-like tetragon solution, corresponding to a u -channel configuration and analyzed in [6], only the time-like tetragon solution can be relevant. All other classes have either not enough cusps or their boundary contains points which are antipodal in AdS_3 . Antipodes in $\text{AdS}_3 \subset \text{AdS}_5$ are automatically antipodes in AdS_5 . The antipodal property is invariant under $O(2, 4)$, hence there is no choice of Poincaré patches in AdS_5 , such that the whole boundary of the surface fits in the conformal image of four-dimensional Minkowski space.

In the time-like tetragon one pair of opposite cusps is time-like and the other one space-like separated. It corresponds to a s -channel scattering configuration. Seemingly there is no corresponding minimal surface in pure AdS_5 . The area for the space-like tetragon case has been calculated in [6]. Let us sketch the corresponding calculation for the time-like tetragon.

We start with (2.88) after some trivial renaming

$$Y^{0'} = \sinh \theta \sinh \eta, \quad Y^0 = \cosh \theta \cosh \xi, \quad Y^1 = \cosh \theta \sinh \xi, \quad Y^2 = \sinh \theta \cosh \eta \quad (5.1)$$

and $Y^4 = Y^3 = 0$. By the application of isometry transformations in $\text{AdS}_4 \subset \text{AdS}_5$ we can generate a boundary configuration related to a generic scattering kinematics. Y^4 will be untouched during this procedure.

Let us consider the two $\text{SO}(2,3)$ matrices

$$A = \begin{pmatrix} 1 & 0 & 0 & 0 & 0 \\ 0 & \frac{1+a^2}{2a} & 0 & 0 & \frac{1-a^2}{2a} \\ 0 & 0 & 1 & 0 & 0 \\ 0 & 0 & 0 & 1 & 0 \\ 0 & \frac{1-a^2}{2a} & 0 & 0 & \frac{1+a^2}{2a} \end{pmatrix}, \quad B = \begin{pmatrix} 1 & 0 & 0 & 0 & 0 \\ 0 & 1 & 0 & 0 & 0 \\ 0 & 0 & 1 & 0 & 0 \\ 0 & 0 & 0 & \frac{1}{\sqrt{1+b^2}} & \frac{-b}{\sqrt{1+b^2}} \\ 0 & 0 & 0 & \frac{b}{\sqrt{1+b^2}} & \frac{1}{\sqrt{1+b^2}} \end{pmatrix}. \quad (5.2)$$

Calculating $A^I{}_J \cdot B^J{}_K \cdot Y^K$ and then introducing Poincaré coordinates (r, y^μ) , $\mu \in \{0', 1, 2\}$ via

$$Y^\mu = \frac{y^\mu}{r}, \quad Y^0 + Y^3 = \frac{1}{r}, \quad Y^0 - Y^3 = \frac{r^2 + y_\mu y^\mu}{r}, \quad (5.3)$$

we find that

$$r = \frac{a\sqrt{1+b^2}}{\sqrt{1+b^2} \cosh \theta \cosh \xi + b \sinh \theta \cosh \eta}, \quad y^{0'} = \frac{a\sqrt{1+b^2} \sinh \theta \sinh \eta}{\sqrt{1+b^2} \cosh \theta \cosh \xi + b \sinh \theta \cosh \eta},$$

$$y^1 = \frac{a\sqrt{1+b^2} \cosh \theta \sinh \xi}{\sqrt{1+b^2} \cosh \theta \cosh \xi + b \sinh \theta \cosh \eta}, \quad y^2 = \frac{a \sinh \theta \cosh \eta}{\sqrt{1+b^2} \cosh \theta \cosh \xi + b \sinh \theta \cosh \eta}. \quad (5.4)$$

Examining (5.1) we see that the cusps are approached by taking either ξ or η constant and sending the other variable to $\pm\infty$. These limits are θ -independent. Thus we find the cusps located at (see fig. 6)

$$\vec{c}_1 = \left(-\frac{a\sqrt{1+b^2}}{b}, 0, \frac{a}{b} \right), \quad \vec{c}_2 = (0, a, 0), \quad \vec{c}_3 = \left(\frac{a\sqrt{1+b^2}}{b}, 0, \frac{a}{b} \right), \quad \vec{c}_4 = (0, -a, 0), \quad (5.5)$$

with $\vec{c} = (y^{0'}, y^1, y^2)$. It can be easily checked that the edges of the tetragon are light-like. The momenta associated with the edges of the tetragon are defined by $2\pi k^\mu = \Delta c^\mu$. In this way we get

$$k_1 = \frac{1}{2} (\sqrt{s}, \sqrt{-t}, -\sqrt{-u}), \quad k_2 = \frac{1}{2} (\sqrt{s}, -\sqrt{-t}, \sqrt{-u}),$$

$$k_3 = \frac{1}{2} (-\sqrt{s}, -\sqrt{-t}, -\sqrt{-u}), \quad k_4 = \frac{1}{2} (-\sqrt{s}, \sqrt{-t}, \sqrt{-u}). \quad (5.6)$$

Here (s, t, u) are the Mandelstam variables, which are related to the parameters (a, b) by

$$s = -2k_1 \cdot k_2 = \frac{a^2(1+b^2)}{\pi^2 b^2}, \quad -t = 2k_1 \cdot k_4 = \frac{a^2}{\pi^2}, \quad -u = 2k_1 \cdot k_3 = \frac{a^2}{\pi^2 b^2}. \quad (5.7)$$

To calculate the regularized action, we introduce a constant cutoff at $r = r_c$ in Poincaré coordinates. Terms that vanish for $r_c \rightarrow 0$ will be discarded. The metric tensor on the surface (including by both AdS_3 and S^3 parts) reads

$$g_{ab}(\sigma, \tau) = f_{ab} + (f_s)_{ab} = (\rho^2 + \rho_s^2) \delta_{ab}. \quad (5.8)$$

Then the regularized action (2.9) is given by

$$S_{reg} = \frac{\sqrt{\lambda}}{2\pi} (\rho^2 + \rho_s^2) \int_{r \geq r_c} d\tau d\sigma . \quad (5.9)$$

The integral runs over that part of the (σ, τ) - plane where $r \geq r_c$. In the (ξ, η) - plane this area is bounded by the contour

$$\epsilon \cosh \eta + \epsilon' \sinh \xi = 1, \quad (5.10)$$

with

$$\epsilon = \frac{\sinh \theta}{\pi \sqrt{s}}, \quad \epsilon' = \frac{\cosh \theta}{\pi \sqrt{-t}}, \quad (5.11)$$

and we can rewrite (5.9) as

$$S_{reg} = \frac{\sqrt{\lambda}}{2\pi} (\rho^2 + \rho_s^2) 2 \mathcal{J} \cdot I(r_c) . \quad (5.12)$$

Here \mathcal{J} is the Jacobian of the linear map between the (ξ, η) and (σ, τ) coordinates and

$$I(r_c) = \frac{1}{2} \int_{r \geq r_c} d\eta d\xi . \quad (5.13)$$

The dependence of $I(r_c)$ on ϵ and ϵ' can be taken from [6]. Inserting the new definitions from (5.11) we find

$$I(r_c) = \frac{1}{4} \left(\log \frac{r_c^2 \sinh^2 \theta}{4\pi^2 s} \right)^2 + \frac{1}{4} \left(\log \frac{r_c^2 \cosh^2 \theta}{-4\pi^2 t} \right)^2 - \frac{1}{4} \left(\log \frac{s \coth^2 \theta}{-t} \right)^2 - \frac{\pi^2}{3} . \quad (5.14)$$

With the Jacobian defined by (2.86) this yields

$$S_{reg} = \frac{\sqrt{\lambda} (\rho^2 + \rho_s^2) \sinh 2\theta}{2\pi \rho \sqrt{1 - \rho^2}} I(r_c) . \quad (5.15)$$

Formally this expression for S_{reg} can also be obtained from the corresponding formula for the space-like tetragon in [6] by $\theta \rightarrow i\theta$ and continuation of ρ^2 (remember footnote 4) from values above 1 to below 1. For the space-like case it was found, that the factor in front of $I(r_c)$ is always ≥ 1 and approaches its lower bound for $\theta \rightarrow \frac{\pi}{4}$, $\rho^2 \rightarrow \infty$ and $\rho_s \rightarrow 0$. In addition, for $\theta = \frac{\pi}{4}$, $I(r_c)$ coincides with the pure AdS case.

Now the situation is different. To analyze the prefactor in (5.15) we use the inequality

$$\sinh 2\theta(\rho, \phi) \geq \sinh 2\theta(\rho, \pi/4) = \frac{2\rho\sqrt{1 - \rho^2}}{2\rho^2 - 1} . \quad (5.16)$$

which follows from (2.87). Setting $\rho_s = 0$ and $\sinh 2\theta$ to its minimal value one finds the prefactor $2\rho^2/(2\rho^2 - 1)$, which is > 2 in the interval $\rho \in (1/2, 1)$. It approaches its lower bound 2 for $\rho^2 \rightarrow 1$. This implies $\theta \rightarrow 0$, which leads to a divergence of $I(r_c)$. Therefore, altogether the meaning of (5.15) for the correspondence to scattering amplitudes remains unclear.

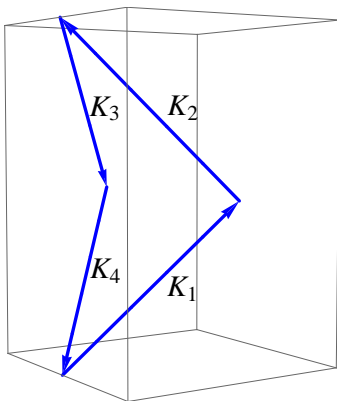


Figure 6: The time-like tetragon configuration in Minkowski space corresponding to s -channel scattering.

6 Conclusions

We have considered the subset of space-like minimal surfaces in $\text{AdS}_3 \times \text{S}^3$, defined by the requirement that they admit constant induced metric for both projections to AdS_3 and S^3 . For almost all cases this leads also to constant second fundamental form, justifying the name vacuum solutions. There is one exceptional case for light-like AdS_3 projection, in which the parameterization needs a free field with unit mass. It would be interesting to further study this integrable subset of solutions.

For all the vacuum solutions a classification and explicit construction has been achieved. Up to the freedom of isometries in $\text{AdS}_3 \times \text{S}^3$, they are parameterized by four parameters ρ , ϕ , ρ_s , ϕ_s . In terms of these parameters one can express the constant mean curvatures of the projections of the surface to AdS_3 ⁸ and S^3 , respectively, as well as the constant ratios of the areas measured with the induced metrics of the projections to the area measured with the metric induced from the total space $\text{AdS}_3 \times \text{S}^3$. For all values of ρ , ϕ , ρ_s , ϕ_s explicit formulæ for the embedding coordinates of the surfaces have been presented.

The projection to S^3 is always a space-like torus. The projection to AdS_3 can be space-like, time-like or light-like. For the space-like case there is only one class of projections, it has the same null tetragonal boundary behavior as the pure AdS_3 solution of [3, 1].

In the time-like case one finds various different classes. Except for one class which stays completely inside, the surfaces touch the conformal boundary of AdS_3 at null lines. Concerning their boundary behavior, the classes are distinguished by counting the corresponding null lines in $\partial\text{AdS}_3 = \text{S}^1 \times \text{S}^1$ (or $\mathbb{R} \times \text{S}^1$). The boundary is part of either one null line, two with the same orientation, two with opposite orientation, three, or four with pairwise opposite orientation.

In the case of light-like projections there are two different classes. One reaches the AdS_3 boundary at a null two-gon built out of a left and a right going null line. The other one reaches the AdS_3 boundary only at a wedge out of pieces of two null lines, but the boundary of the surfaces AdS_3 projection is completed by a line inside AdS_3 .

⁸For surfaces with constant mean curvature in pure AdS see [11].

Altogether nine different classes are related to different pieces of the (ρ, ϕ) -diagram. Since ρ and ϕ carry information both on the shape of the projection in pure AdS₃-sense (mean curvature) as well as information on the relation to the surface in the total product space, AdS₃ projections with the same shape are situated on curves in the (ρ, ϕ) -diagram.

All AdS₃ projections can be described as (parts of) intersections of quadrics with the AdS-hyperboloid. In each class we have chosen a canonical form of the intersecting quadric and plotted the resulting surfaces. All other AdS₃-projections can be reached from these pictures by varying the inhomogeneity parameters of these forms and/or applying O(2, 2) isometry transformations.

While isometry transformations of course do not touch the geometric shape, they can change the apparent shape relative to a chosen coordinate system. We have discussed, how just in this sense one can approach some classes in the limit of infinite boosts from other classes

We made the observation that our surfaces can be related to solutions of the complex sin(h)-Gordon type equations, which for the light-like surfaces degenerate to a linear equation.

For potential use in the correspondence to gluon scattering amplitudes we have calculated the regularized area of the surface with a generic s -channel null tetragon boundary, i.e. two non-consecutive cusps with space-like and two with time-like separation. This configuration is remarkable, because there is no corresponding solution in the pure AdS case. The standard tetragon of [3, 1] is relevant for the u -channel case, where all four cusps have space-like momentum sum.

Finally, a corresponding classification of vacuum type time-like strings can be similarly carried out (as it was pointed out in [6]).

Acknowledgments

We thank Johannes Henn, Jan Plefka, Donovan Young and especially Nadav Drukker for useful discussions.

This work has been supported in part by Deutsche Forschungsgemeinschaft via SFB 647 and by VolkswagenStiftung. G.J. was also supported by GNSF.

A Useful formulæ

Here we present some useful formulæ for the SU(2) and SL(2, ℝ) groups.

A.1 SU(2) group

Using the $\mathfrak{su}(2)$ algebra (2.6) one gets $\mathbf{u}^2 = -(u_n u_n) \mathbf{I}$, for any $\mathbf{u} = u_n \mathbf{s}_n \in \mathfrak{su}(2)$, and then

$$e^{\mathbf{u}} = \cos u I + \sin u \hat{\mathbf{u}} , \quad \text{with } u = \sqrt{u_n u_n} , \quad \hat{\mathbf{u}} = \mathbf{u}/u . \quad (\text{A.1})$$

In particular,

$$e^{i\theta\sigma_2} = \begin{pmatrix} \cos\theta & \sin\theta \\ -\sin\theta & \cos\theta \end{pmatrix}, \quad e^{i\eta\sigma_3} = \begin{pmatrix} e^{i\eta} & 0 \\ 0 & e^{-i\eta} \end{pmatrix}, \quad (\text{A.2})$$

and the SO(2) adjoint orbit of \mathbf{s}_3 generated by \mathbf{s}_2 is given by

$$e^{-i\beta\sigma_2} \mathbf{s}_3 e^{i\beta\sigma_2} = \cos 2\beta \mathbf{s}_3 + \sin 2\beta \mathbf{s}_1. \quad (\text{A.3})$$

With these equations and the identity

$$e^{(e^{\mathbf{u}} \mathbf{v} e^{-\mathbf{u}})} = e^{\mathbf{u}} e^{\mathbf{v}} e^{-\mathbf{u}}, \quad (\text{A.4})$$

one easily obtains (2.38)-(2.39).

A.2 $\mathbf{SL}(2, \mathbb{R})$ group

From (2.5) follows $\mathbf{a}^2 = \langle \mathbf{a} \mathbf{a} \rangle \mathbf{I}$, for any $\mathbf{a} \in \mathfrak{sl}(2, \mathbb{R})$. In particular, if $\langle \mathbf{a} \mathbf{a} \rangle = 0$, then \mathbf{a} is nilpotent $\mathbf{a}^2 = 0$. A compact form of the exponent $e^{\mathbf{a}}$ then reads

$$\begin{aligned} e^{\mathbf{a}} &= \cosh \theta \mathbf{I} + \frac{\sinh \theta}{\theta} \mathbf{a}, & \text{with } \theta &= \sqrt{\langle \mathbf{a} \mathbf{a} \rangle}, & \text{if } \langle \mathbf{a} \mathbf{a} \rangle > 0; \\ e^{\mathbf{a}} &= \cos \theta \mathbf{I} + \frac{\sin \theta}{\theta} \mathbf{a}, & \text{with } \theta &= \sqrt{-\langle \mathbf{a} \mathbf{a} \rangle}, & \text{if } \langle \mathbf{a} \mathbf{a} \rangle < 0; \\ e^{\mathbf{a}} &= \mathbf{I} + \mathbf{a}, & & & \text{if } \langle \mathbf{a} \mathbf{a} \rangle = 0. \end{aligned} \quad (\text{A.5})$$

One gets the following one parameter subgroups

$$e^{\theta \mathbf{t}_0} = \begin{pmatrix} \cos \theta & \sin \theta \\ -\sin \theta & \cos \theta \end{pmatrix}, \quad e^{\theta \mathbf{t}_1} = \begin{pmatrix} \cosh \theta & \sinh \theta \\ \sinh \theta & \cosh \theta \end{pmatrix}, \quad e^{\theta \mathbf{t}_-} = \begin{pmatrix} 1 & 0 \\ \theta & 1 \end{pmatrix}, \quad (\text{A.6})$$

with $\mathbf{t}_- = \frac{1}{2}(\mathbf{t}_1 - \mathbf{t}_0)$, and the corresponding adjoint orbits of \mathbf{t}_2 are

$$e^{-\theta \mathbf{t}_0} \mathbf{t}_2 e^{\theta \mathbf{t}_0} = \cos 2\theta \mathbf{t}_2 + \sin 2\theta \mathbf{t}_1, \quad e^{-\theta \mathbf{t}_1} \mathbf{t}_2 e^{\theta \mathbf{t}_1} = \cosh 2\theta \mathbf{t}_2 + \sinh 2\theta \mathbf{t}_0, \quad (\text{A.7})$$

$$e^{-\theta \mathbf{t}_+} \mathbf{t}_2 e^{\theta \mathbf{t}_+} = \mathbf{t}_2 + 2\theta \mathbf{t}_+. \quad (\text{A.8})$$

The following summation rules become helpful in calculations

$$\epsilon_{\mu\nu\rho} \epsilon_{\mu'\nu'}{}^\rho = \eta_{\mu\nu'} \eta_{\nu\mu'} - \eta_{\mu\mu'} \eta_{\nu\nu'}, \quad (\text{A.9})$$

$$(\mathbf{t}_\mu)_{a\dot{a}} (\mathbf{t}^\mu)_{b\dot{b}} = 2\delta_{ab} \delta_{\dot{a}\dot{b}} - \delta_{a\dot{a}} \delta_{b\dot{b}}. \quad (\text{A.10})$$

B Left-right decomposition of $\mathfrak{so}(2, 2)$

Let us consider the map $\mathcal{M} : \mathbb{R}^{2,2} \mapsto \mathfrak{gl}(2, \mathbb{R})$ given by

$$S_{a\dot{a}} = Y^{0'} \delta_{a\dot{a}} + Y^\mu (\mathbf{t}_\mu)_{a\dot{a}}. \quad (\text{B.1})$$

Here $S_{a\dot{a}} \in \mathfrak{gl}(2, \mathbb{R})$ is a 2×2 matrix and $(Y^{0'}, Y^\mu)$ ($\mu = 0, 1, 2$) are coordinates of $Y \in \mathbb{R}^{2,2}$. We also use Y^J , $J = (0', 0, 1, 2)$ and treat it as a row. A matrix of a linear transformation acts then on Y^J from the r.h.s. The inverse map takes the form $Y^{0'} = \langle S \rangle$, $Y_\mu = \langle \mathbf{t}_\mu S \rangle$. Writing these linear maps in the matrix form $S_{a\dot{a}} = Y^J M_{J, a\dot{a}}$, $Y_J = S_{a\dot{a}} M_{a\dot{a}, J}^{-1}$, one gets the matrix components

$$\begin{aligned} M_{0', a\dot{a}} &= \delta_{a\dot{a}} , & M_{\mu, a\dot{a}} &= (\mathbf{t}_\mu)_{a\dot{a}} , \\ M_{a\dot{a}, 0'}^{-1} &= -\frac{1}{2} \delta_{a\dot{a}} , & M_{a\dot{a}, \mu}^{-1} &= \frac{1}{2} (\mathbf{t}_\mu)_{\dot{a}a} . \end{aligned} \quad (\text{B.2})$$

With the help of the identity (A.9) one can check that

$$Y \cdot Z = \langle ST \rangle - 2 \langle S \rangle \langle T \rangle , \quad (\text{B.3})$$

where $Y \cdot Z = Y^J Z_J$ is the inner product in $\mathbb{R}^{2,2}$, $S = \mathcal{M}(Y)$ and $T = \mathcal{M}(Z)$. The bilinear form (B.3) makes $\mathfrak{gl}(2, \mathbb{R})$ isometric to $\mathbb{R}^{2,2}$. This inner product⁹ is invariant under the infinitesimal left and right multiplications

$$S \mapsto S + \epsilon^\mu \mathbf{t}_\mu S , \quad S \mapsto S - \epsilon^\mu S \mathbf{t}_\mu . \quad (\text{B.4})$$

The linear transformations in $\mathfrak{gl}(2, \mathbb{R})$: $S \mapsto \mathbf{t}_\mu S$ and $S \mapsto -S \mathbf{t}_\mu$ are given by the matrices

$$(\hat{L}_\mu)_{bb, a\dot{a}} = (\mathbf{t}_\mu)_{ab} \delta_{\dot{b}\dot{a}} , \quad (\hat{R}_\mu)_{bb, a\dot{a}} = -\delta_{ba} (\mathbf{t}_\mu)_{\dot{b}\dot{a}} . \quad (\text{B.5})$$

By (B.2) and (B.5), the corresponding matrices in $\mathbb{R}^{2,2}$

$$(L_\mu)_{JK} = M_{J, b\dot{b}} (\hat{L}_\mu)_{b\dot{b}, a\dot{a}} M_{a\dot{a}, K}^{-1} , \quad (R_\mu)_{JK} = M_{J, b\dot{b}} (\hat{R}_\mu)_{b\dot{b}, a\dot{a}} M_{a\dot{a}, K}^{-1} . \quad (\text{B.6})$$

become

$$\begin{aligned} (L_\mu)_{0'0'} &= 0 , & (L_\mu)_{0'\nu} &= \eta_{\mu\nu} , & (L_\mu)_{\nu 0'} &= -\eta_{\mu\nu} , & (L_\mu)_{\nu\nu'} &= \epsilon_{\mu\nu\nu'} , \\ (R_\mu)_{0'0'} &= 0 , & (R_\mu)_{0'\nu} &= -\eta_{\mu\nu} , & (R_\mu)_{\nu 0'} &= \eta_{\mu\nu} , & (R_\mu)_{\nu\nu'} &= \epsilon_{\mu\nu\nu'} , \end{aligned} \quad (\text{B.7})$$

and one obtains (3.19).

Now we consider the matrix exponent

$$\mathcal{E}_J^K = \left(e^{l^\mu L_\mu + r^\nu R_\nu} \right)_J^K , \quad (\text{B.8})$$

where l^μ , r^ν are 3d Minkowski vectors and L_μ , R_ν are the basis vectors (3.19). The exponent in (3.22) is a particular case of (B.8). The map of the first row of (B.8) to $\text{SL}(2, \mathbb{R})$, defined by (B.1) can be written as

$$g_{a\dot{a}} = \mathcal{E}_{0'}^K M_{K, a\dot{a}} = \left(e^{l^\mu \hat{L}_\mu} e^{r^\nu \hat{R}_\nu} \right)_{bb, a\dot{a}} , \quad (\text{B.9})$$

with \hat{L}_μ , \hat{R}_μ , given by (B.5). Using (B.5), we obtain

$$g_{a\dot{a}} = \left(e^{l^\mu \mathbf{t}_\mu} \right)_{cb} \delta_{b\dot{c}} \delta_{ac} \left(e^{-r^\nu \mathbf{t}_\nu} \right)_{\dot{c}\dot{a}} = \left(e^{l^\mu \mathbf{t}_\mu} \right)_{ab} \left(e^{-r^\nu \mathbf{t}_\nu} \right)_{\dot{b}\dot{a}} . \quad (\text{B.10})$$

Taking l_μ , r_ν corresponding to (3.22), from (B.10) we find the factorized form of the g -field (2.50).

⁹Note that this inner product differs from the standard Killing form on $\mathfrak{gl}(2, \mathbb{R})$, which is degenerated.

References

- [1] L. F. Alday and J. M. Maldacena, “*Gluon scattering amplitudes at strong coupling*,” JHEP **0706**, 064 (2007) [arXiv:0705.0303 [hep-th]].
- [2] L. F. Alday and J. Maldacena, “*Comments on gluon scattering amplitudes via AdS/CFT*,” JHEP **0711** (2007) 068 [arXiv:0710.1060 [hep-th]].
L. F. Alday, “*Lectures on Scattering Amplitudes via AdS/CFT*,” Fortsch. Phys. **56**, 816 (2008) [arXiv:0804.0951 [hep-th]].
L. F. Alday and J. Maldacena, “*Null polygonal Wilson loops and minimal surfaces in Anti-de-Sitter space*,” JHEP **0911** (2009) 082 [arXiv:0904.0663 [hep-th]].
L. F. Alday, D. Gaiotto and J. Maldacena, “*Thermodynamic Bubble Ansatz*,” [arXiv:0911.4708 [hep-th]].
L. F. Alday, J. Maldacena, A. Sever and P. Vieira, “*Y-system for Scattering Amplitudes*,” [arXiv:1002.2459 [hep-th]].
- [3] M. Kruczenski, “*A note on twist two operators in $\mathcal{N} = 4$ SYM and Wilson loops in Minkowski signature*,” JHEP **0212** (2002) 024 [arXiv:0210115 [hep-th]].
- [4] H. Dorn, G. Jorjadze and S. Wuttke, “*On space-like and time-like minimal surfaces in AdS_n* ,” JHEP **0905** (2009) 048 [arXiv:0903.0977 [hep-th]].
- [5] G. Arutyunov and S. Frolov, “*Foundations of the $AdS_5 \times S^5$ Superstring. Part I*,” J. Phys. A **42** (2009) 254003 [arXiv:0901.4937 [hep-th]].
- [6] H. Dorn, N. Drukker, G. Jorjadze and C. Kalousios, “*Space-like minimal surfaces in $AdS \times S$* ,” JHEP **1004**, 004 (2010) [arXiv:0912.3829 [hep-th]].
- [7] K. Sakai and Y. Satoh, “*A note on string solutions in AdS_3* ,” JHEP **0910**, 001 (2009) arXiv:0907.5259 [hep-th].
- [8] K. Pohlmeyer, “*Integrable Hamiltonian Systems And Interactions Through Quadratic Constraints*,” Commun. Math. Phys. **46**, 207 (1976).
H. J. De Vega and N. G. Sanchez, “*Exact Integrability Of Strings In D-Dimensional De Sitter Space-Time*,” Phys. Rev. D **47** (1993) 3394.
M. Grigoriev and A. A. Tseytlin, “*Pohlmeyer reduction of $AdS_5 \times S^5$ superstring sigma model*,” Nucl. Phys. B **800** (2008) 450 [arXiv:0711.0155 [hep-th]].
A. Jevicki, K. Jin, C. Kalousios and A. Volovich, “*Generating AdS String Solutions*,” JHEP **0803** (2008) 032 [arXiv:0712.1193 [hep-th]].
J. L. Miramontes, “*Pohlmeyer reduction revisited*,” JHEP **0810** (2008) 087 [arXiv:0808.3365 [hep-th]].
- [9] J. M. Maldacena and H. Ooguri, “*Strings in AdS_3 and $SL(2, \mathbb{R})$ WZW model. I: The Spectrum*,” J. Math. Phys. **42**, 2929 (2001) [arXiv:hep-th/0001053].
- [10] G. Jorjadze, “*Singular Liouville fields and spiky strings in $\mathbb{R}^{1,2}$ and $SL(2, \mathbb{R})$* ,” JHEP **0910** (2009) 092 [arXiv:0909.0350 [hep-th]].
- [11] K. Sakai and Y. Satoh, “*Constant mean curvature surfaces in AdS_3* ,” JHEP **1003**, 077 (2010) [arXiv:1001.1553 [hep-th]].